AFFDL-TR-69-50

AD-715331

CRACK PROPAGATION IN ALUMINUM ALLOY SHEET MATERIALS UNDER FLIGHT SIMULATION LOADING

J. SCHIJVE, F. A. JACOBS AND P. J. TROMP

NATIONAL AEROSPACE LABORATORY, NLR

AMSTERDAM

TECHNICAL REPORT AFFDL-TR-69-50

SEPTEMBER 1970

This document has been approved for public release and sale; its distribution is unlimited.

AIR FORCE FLIGHT DYNAMICS LABORATORY
AIR FORCE SYSTEMS COMMAND
WRIGHT-PATTERSON AIR FORCE BASE, OHIO

20071128030

NOTICE

When Government drawings, specifications, or other data are used for any purpose other than in connection with a definitely related Government procurement operation, the United States Government thereby incurs no responsibility nor any obligation whatsoever; and the fact that the government may have formulated, furnished, or in any way supplied the said drawings, specifications, or other data, is not to be regarded by implication or otherwise as in any manner licensing the holder or any other person or corporation, or conveying any rights or permission to manufacture, use, or sell any patented invention that may in any way be related thereto.

Copies of this report should not be returned unless return is required by security considerations, contractual obligations, or notice on a specific document.

200-October 1970-CO305-8-71-162

CRACK PROPAGATION IN ALUMINUM ALLOY SHEET MATERIALS UNDER FLIGHT SIMULATION LOADING

J. SCHIJVE, F. A. JACOBS AND P. J. TROMP

NATIONAL AEROSPACE LABORATORY, NLR
AMSTERDAM

This document has been approved for public release
and sale; its distribution is unlimited.

FOREWORD

This report, prepared by the National Aerospace Laboratory, NLR, Amsterdam, Metherlands, covers the work performed under Air Force Contract F61052 67 C 0076, "Crack Propagation in Aluminum Alloy Sheet Materials Under Flight Simulation Loading". The program was administered under the direction of the Air Force Flight Dynamics Laboratory by Mr. William R. Johnston, Experimental Branch (FDTT), Structures Division, Project Engineer.

The work covered by this report was performed during the period from February 1967 to December 1968.

This technical report has been reviewed and is approved.

Robert L. Cavanagh

ROBERT L. CAVANAGH
Chief, Experimental Branch
Structures Division
AF Flight Dynamics Laboratory

ABSTRACT

A large number of flight-simulation tests were carried out on sheet specimens of 7C75-T6 and 2024-T3 clad material. A gust load spectrum was adopted and a flight-by-flight loading was applied. The investigation is essentially concerned with macro-crack propagation although a few exploratory tests were conducted on the crack nucleation period. The major trends emerging from tests with a variety of loading programs are:

(1) The omission of taxiing loads from the ground to air cycles did not affect the crack propagation.

(2) The sequence of the gust cycles in a flight (random, programmed, reversed gust cycles) did not have a significant influence on the crack propagation.

(3) Omission of gust cycles with small amplitudes systematically increased the crack propagation life.

(4) The most predominant effect on the crack propagation was coming from the maximum gust amplitude included in the test. Increasing this amplitude gave a large increase of the crack propagation life.

(5) Application in each flight of a single gust load only, namely the largest upward gust load, increased the crack propagation life three times.

(6) Omission of the ground-to-air cycle increased the life 1.5-1.8 times.

The discussion and the analysis of the results include such aspects as fractographic analysis, possible **mechanisms** for interaction effects between load cycles of different magnitudes and damage calculations. The conclusions at the end of the report have a number of implications for testing procedures to be applied in full-scale testing aiming at crack propagation data for fail-safe considerations. A recommendation is made for selecting the maximum load level in such a test. Recommendations for further study are also made.

Table of Contents

	Page
Abstract	iii
List of abbreviations and symbols	iv
List of illustrations	v
List of tables	vi
1. Introduction	1
2. Survey and scope of the test series	2
3. Materials and specimens	4
4. Experimental procedures	4
4.1 The anti-buckling guides	4
4.2 The fatigue apparatus	5
4.3 The crack propagation tests	6
5. The fatigue loads	6
5.1 The gust loads	6
5.2 The ground-to-air cycles and the taxiing loads	8
6. Test results	8
6.1 Results of the flight-simulation tests	8
6.2 Results of the constant-amplitude tests and damage calculations	9
6.3 Results of the tests on specimens with a central hole	10
6.4 Some fractographic observations	11
7. Analysis of the present results and comparison with data from the literature	13
7.1 Interaction between load cycles of different magnitudes	13
7.2 The omission of the taxiing loads (TL) from the ground-to-air cycle (GTAC)	15
7.3 The minimum stress of the GTAC	15
7.4 Omission of the small gust loads	16
7.5 The effect of the gust cycles with a high amplitude	18
7.6 Random or programmed gust sequences in each flight and reversion of the gust cycle	19
7.7 Application of a single gust load per flight	21
7.8 Omission of the GTAC	21
7.9 Comparison between the two alloys, 7075 and 2024	22
7.10 Damage calculations	22
8. Discussion	23
8.1 Recommendation for the maximum load in a flight-simulation test	23
8.2 Alternatives to flight-simulation	24
8.3 Suggestions for further work	25

	Page
9. Conclusions	26
10. List of references	28

19 tables

19 figures

List of Illustrations.

Fig. 1 Survey of variables studied in the present test series.

Fig. 2 The load sequence in the most severe flight (type A).

Fig. 3 Load records of flight No. 19 (Type F) for different types of flight simulation.

Fig. 4 Dimensions of the specimen and anti-buckling guides.

Fig. 5 Picture of the specimen, anti-buckling guides with window and clampings. Stereo-microscope (30x) for crack observation in the background.

Fig. 6 Two specimens connected by a double strap joint, anti-buckling guides covered by felt at the inner side and provided with two windows each.

Fig. 7 Example of two crack propagation curves for two specimens simultaneously tested in series.

Fig. 8 Effect of truncation ($S_{a,max}$) on the crack propagation rate material 7075-T6.

Fig. 8 continued. Material 2024-T3.

Fig. 9 Effect of omitting small gust loads on the crack propagation rate material 7075-T6.

Fig. 9 continued. Material 2024-T3.

Fig.10 The effects of omitting the GTAC and of reversing the gust cycles on the crack propagation rate.

Fig.11 Comparison between the crack rates for random and programmed flight simulation.

Fig.12 Comparison between the crack rates in the two alloys.
Effect of $S_{a,max}$ and $S_{a,min}$, see also fig. 11.
Random gusts, GTAC without TL, $S_{min} = -3.4$.

Fig.13 The effect of omitting small gust loads on the crack propagation life.

Fig.14 The effect of truncating the gust load spectrum on the crack propagation life.

Fig.15 The constant-amplitude test data plotted as S-N curves.

Fig.16 Crack propagation curves for the 2024-T3 specimens with a central hole
Effect of truncation level ($S_{a,max}$) on the crack-nucleation period (to $\ell' = 2$ mm) and the crack propagation life.

Fig. 17 Comparison between the crack propagation rates in specimens with a small notch or a central hole.

Fig.18 Fracture surfaces of 4 specimens showing macro fatigue bands.

Fig. 19 Two examples of fatigue striations as observed by the electron microscope.

List of Tables.

Table 1 Survey of the test parameters in the various test series.

Table 2 Survey of the flight-simulation tests on sheet specimens with a central hole.

Table 3 Survey of the constant-amplitude tests.

Table 4 Static properties of the materials.

Table 5 Gust load occurrences in the 10 different types of flights.

Table 6 Diagrammatic picture of the sequence of the various flights in 5000 flights.

Table 7 Crack propagation records of the flight-simulation tests. Values of Δn in numbers of flights.

Table 8 Crack propagation records of the additional flight-simulation tests. Values of Δn in numbers of flights.

Table 9 Crack propagation records of the constant-amplitude tests. Values of Δn in cycles.

Table 10 Crack propagation records for the 2024-T3 specimens with a central hole.

Table 11 Effect of taxiing loads.

Table 12 Effect of the minimum stress in the GTAC.

Table 13 Effect of omitting small gust loads.

Table 14 Effect of truncating the gust spectrum.

Table 15 Comparison between the random and the programmed flight simulation tests.

Table 16 Effects of reversing the gust cycles, of applying one gust per flight and of omitting the GTAC.

Table 17 Comparison between the two alloys.

Table 18 Damage calculations for test series No. 45.

Table 19 Fatigue life reduction if small gust cycles are included.

List of Abbreviations and Symbols

CTAC	ground to air cycle (in the literature sometimes: GAC = ground-air-ground transition)
TL	taxiing loads

Crack propagation life: number of flights for crack growth from ℓ = 10 mm to complete failure of the specimen.

ℓ	semi crack length, see fig.4
n	number of flights (or cycles)
$d\ell/dn$	crack propagation rate
Δn	number of flights (or cycles) to cover the crack growth interval from ℓ_i to ℓ_{i+1}
N	crack propagation life, or fatigue life

S_a	stress amplitude	gross stress (in kg/mm^2 if not specified otherwise)
S_m	mean stress	
S_{min}	minimum stress	
S_{max}	maximum stress	
$S_{a,min}$	minimum S_a of the gust cycles	
$S_{a,max}$	maximum S_a of the gust cycles	

1 mm = 10^{-3} meter = 0.04 inch; 1 inch = 25.4 mm

1 kg/mm^2 = 1,422 psi ; 1000 psi = 0.703 kg/mm^2

1 kc = 1 kilocycle = 1000 cycles

1 μ/fl. = crack rate of 1 micron (10^{-6} meter) per flight

1 Introduction.

Full-scale fatigue testing at the present time is generally accepted as a useful procedure, if not the only one, for evaluating the fatigue qualities of an aircraft structure. Major goals to be achieved are:

(a) Indication of structural deficiencies, fatigue critical elements.
(b) Determination of fatigue lives until visible cracking occurs,
(c) Determination of crack propagation rates in view of inspections.
(d) Evaluation of inspection procedures.
(e) Measurements on residual strength.

In order to obtain realistic data on (b) and (c) it will be clear that the fatigue loads to be applied in a full-scale test should be a realistic representation of the load-time history in service. This problem was extensively discussed in ref.1, which was the Final Report of a preceding investigation. It was concluded in this report that the load sequence should have the character of a flight by flight simulation. This conclusion still leaves various questions to be answered, such as:

(1) The sequence of loads within each flight, should it be a random sequence or could a programmed sequence be allowed? A fully randomized sequence and a programmed sequence are thought to be the most extreme possibilities.
(2) What is the maximum load to be applied in the test (truncation of load spectrum)?
(3) Could small load fluctuations be omitted from the test in view of time saving?

These three questions were also extensively discussed in ref.1 and certain recommendations were made. Nevertheless it had to be admitted that more empirical data was urgently desirable.

The present investigation deals with fatigue crack propagation tests on sheet specimens of two aluminum alloys (2024 and 7075). Load sequences were selected in such a way as to shed some further light on the three questions mentioned above. In addition test series were carried out to study the damaging effect of ground-to-air cycles, the effect of reversing the order of positive and negative gusts and the effect of applying only the most severe gust load in each flight. Some constant-amplitude tests were made for damage calculations. A survey of all test series is given in the following chapter.

It should be pointed out that the present test series involves the propagation of visible cracks only. It is thought that the results will be helpful in planning fatigue tests with flight simulation loading on full-scale structures or components, especially if crack propagation has to be studied (fail-safe structures). This report gives a full description of the experiments and the results obtained. The analysis of the data (chapter 7) includes a discussion of related test programs reported in the literature. The report is completed by a general discussion and a number of conclusions.

2 Survey and scope of the test series.

A gust load spectrum was approximated by a stepped function as indicated in fig.1. This spectrum was subsequently broken down into 10 different types of flight (A-K), each characterized by its own load spectrum, varying from "good weather" conditions to "storm" conditions (see chapter 5). The sequence of the various types of flights in the tests was random, while the gusts in each flight were also applied in a random order. A schematic picture of a flight is shown in fig.1 and a load record of the severest flight is presented in fig.2. Each gust cycle consisted of an upward gust load immediately followed by a downward gust load of the same magnitude, the mean stress being 7.0 kg/mm^2 (10.0 ksi). Taxiing loads applied in the ground-to-air cycle (GTAC) or air-ground-air transition had a constant amplitude (S_a = 1.4 kg/mm^2) and the number of these cycles per GTAC was 20.

As outlined in the introduction, the main purpose of the present investigation was a comparative study of several load sequences to be adopted for flight-simulation testing. A summary of the variables studied in the present test program is given in the table in fig.1 and a survey of the test parameters is presented in table 1.

a Truncation of the gust load spectrum. Extremely high gust loads are very rare. Unfortunately they may have a large effect on crack propagation and since one can not be sure that all aircraft of a fleet will meet the same high gust loads it is a delicate issue to assess the maximum load to be applied in a flight simulation test (ref.1). In view of this problem comparative tests were carried out with the maximum gust load level (truncation of load spectrum, see fig.1) as a variable.

b <u>Omission of small gust loads</u>. The omission of small gust load cycles in a flight simulation test would save a considerable amount of time since these cycles are relatively numerous, see fig. 3. Since these cycles may still contribute to crack growth comparative tests were made with and without the smallest gust cycles.

c <u>S_{min} in the GTAC (ground-to-air cycle)</u>. In some exploratory tests S_{min} in the GTAC was -1.4 kg/mm^2 whereas in the major part of the investigation a value of -3.4 kg/mm^2 was adopted. This allows a limited comparison to be made.

d <u>Taxiing loads</u>. Taxiing loads (TL) are superimposed on the GTAC. For a wing structure they are thought to be relatively unimportant for the fatigue life, except for decreasing the minimum stress level in the GTAC (ref. 1). Comparative tests were made to explore this question, since the omission of the taxiing loads implies again an appreciable time saving. Since the present test program confirmed the negligible damage contribution of the taxiing loads these loads were omitted in various test series of the program when studying other variables (see fig. 3).

e <u>Omission of the GTAC</u>. Two test series were carried out without ground-to-air cycles in order to estimate the damaging effect of the GTAC.

f <u>One gust cycle per flight</u>. Flight-simulation tests were carried out with only the largest positive gust load of each flight being applied. It implies that in each flight all smaller gust cycles are omitted except for the positive half of the largest one, see fig. 3. This simplification, implying a further time saving, was based on the idea (ref. 2) that the highest (and the lowest) stress level in a flight will have a predominant effect on the fatigue damage contribution of the flight.

g <u>Reversed random sequence</u>. In the present tests a positive gust load was always followed by a negative gust load of equal magnitude since this was thought to be just slightly conservative (ref.3). The other extreme is that each positive gust load is preceeded by a negative one of equal magnitude. In view of a possible influence two test series were carried out with the sequence of each gust cycle in this reversed sequence, see fig. 3.

h <u>Programmed sequences</u>. Several test series were carried out with programmed gust load sequences, that means that within each flight the gust load cycles were applied in an increasing-decreasing order of amplitudes, see fig. 3. The sequence of the flights, however, remained unchanged. Such a programmed flight simulation may give indications on the importance of load sequences within a flight.

1 Materials. Apart from the exploratory tests almost all load sequences were applied to both 7075-T6 and 2024-T3 specimens. This allows a comparison of the two alloys and in addition it may show whether certain influences are more important for one material than for the other.

A small number of tests were carried out on sheet specimens with a central hole instead of a sharp notch. The aim of these tests was to see whether the significant effect of truncation as found for crack propagation also applies to crack nucleation. These tests on specimens of 2024-T3 material , see table 2, were of an exploratory nature only.

After the completion of the flight-simulation tests,a small number of specimens was still left. These specimens have been used for constant-amplitude tests. The results allow some damage calculations to be made. A survey of these tests is given in table 3.

3 Materials and specimens.

Specimens were cut from 2024-T3 Alclad and 7075-T6 Clad sheet materials. The nominal thickness of the sheets was 2 mm (0.08 inch). The material properties as determined on tensile specimens cut in the longitudinal and transverse direction from the sheets are given in table 4. The results are considered as being typical for these alloys.

The specimens were cut to a width of 160 mm and a length of 235 mm. The free length between the clampings was 160 mm, that is equal to the specimen width, see figure 4. A sharp central notch was made by drilling a small hole and making two short saw cuts at both sides of the hole. The specimens were subsequently pre-cracked to a crack length $\ell = 10$ mm (0.4 in) by cycling between $S_{max} = 10$ kg/mm^2 and $S_{min} = 0$ kg/mm^2. Since the stresses in the flight-simulation tests are beyond these values it was thought that an effect of precracking on subsequent crack growth should be negligible.

4 Experimental procedures.

4.1 The anti-buckling guides.

In order to prevent buckling of the specimens two aluminum alloy plates were

used as anti buckling guides, see fig. 4 and the picture in fig. 5. At the inner side felt was bonded to the plates to minimize the friction between the specimens and the guide plates. Each plate was provided with a window for observation of the crack growth.

The bolts connecting the two plates were hand tightened. The NLR had previously used such a device for riveted joints. Nevertheless it was checked by strain gages whether no load was transmitted through the plates. At the same time these measurements were used to check the stress distribution in the sheet specimen. A dummy specimen without central notch and cracks was provided with three strain gages at each side of the specimen, located at the two ends and the centre of the windows. It turned out that no load transmission through the guide plates could be indicated, provided the bolts were loosely tightened. Moreover sheet bending was practically absent and the stress distribution was satisfactory. Differences between dynamic and static strain readings were in the order of 1 $^{o}/o$ or less. The measurements covered the stress ranges to be applied in the fatigue tests.

After the first preliminary tests were carried out it became desirable to speed up the test program by testing two specimens in series. The specimens are interconnected by two relatively heavy strap plates of steel and a single row of bolts in each specimen. A rigid clamping had to be made since the clamping in the machine itself is also a rigid one. Fig. 6 shows the various parts involved. The anti-buckling guides had to be made larger in order to cover both specimens. Tests were continued until one of the two specimens fractured completely. Since the scatter of the crack rate was low crack growth in the second specimen covered a large part of the cross section.

4.2 The fatigue apparatus.

The specimens are loaded in an MTS fatigue machine, type 901.55, maximum dynamic capacity 25 tons. In this hydraulic machine the load control occurs by an electro-hydraulic servo valve in a closed circuit feed back system. The valve is fed by an electric signal representing the required fatigue load. This signal is generated by a piece of apparatus, called PAGE (Programmed Amplitude GEnerator) developed at the NLR. It employs the function generator of the MTS-machine for producing half sine wave functions. PAGE allows any sequence of half sine waves with different amplitudes to be selected as well as a shift between two selected mean values of the cyclic load. The latter is required in view of the GTAC (ground-to-air cycle). The sequence of amplitudes and the selection of the corresponding mean load is punched into a binary digit tape. A Creed model 92 tape

reader is part of the PAGE apparatus. It further includes a patch board on which the cycling frequency can be set separately for each amplitude. In general a lower frequency will be selected for a large amplitude and vice versa.

A sample of a load sequence (recorded at a low loading rate in view of the recorder) is shown in fig. 2. Load frequencies adopted in the tests are 10 cps for the taxiing loads and the lower gust loads (S_a = 1.1 - 4.4 kg/mm^2) while for the higher gust loads the frequency was inversely proportional to the stress amplitude, varying from 8 to 3.6 cps for S_a from 5.5 to 12.1 kg/mm^2.

4.3 The crack propagation tests.

Pre-cracking of the specimens occurred in an Amsler High Frequency Pulsator (frequency 100 cycles per second). After pre-cracking the specimens were mounted into the MTS machine and flight simulation loading was started. The propagation of the cracks was observed continuously with a magnifying glass or a stereo-microscope (30 x).

The specimens were provided with fine scribe-line markings, see fig. 4. If the tip of a crack just reached such a line the number of flights covered was recorded and these data were used for the evaluation of the crack propagation.

If one specimen of a pair tested in series failed the fatigue life until failure for the other one was obtained by extrapolation of the crack propagation curve employing the data of the fractured specimen, see fig. 7. It will be clear that this will not introduce inaccuracies of any importance. Results obtained did not indicate systematic differences between the results of specimens tested in series and specimens tested separately.

5 The fatigue loads.

5.1 The gust loads.

A gust spectrum was recently derived in the Netherlands from flight data obtained in England, Australia and the USA. The shape of the spectrum is shown in fig. 1. The gust spectrum was converted into a stress spectrum, by using a conversion factor 1ft/sec $\widehat{=}$ 0.3 kg/mm^2 (430 psi), a value frequently adopted by the NLR for program tests. As a mean stress a value S_m = 7.0 kg/mm^2 (10 ksi) was selected.

For the flight simulation tests the load spectrum as given in fig. 1 had to be distributed over a number of different flights. It will be clear that the load spectrum cannot be the same for all flights since the more severe gusts have an average frequency of occurrence of less than once in a flight. Ten different types of flights were designed, each characterized by its own load spectrum varying from "good weather" conditions to "storm" conditions. This was done in such a way that the shape of the load spectrum (statistically speaking: the distribution function) is approximately the same for all flights except for the severety which is different. Justification for this procedure is found in gust load measurements evaluated by Bullen (ref. 4), and in the modern power spectral density conception indicating that the shape of the spectral density function of the gust is invariable but the intensity is depending on weather conditions and flying height (ref.5). Starting from the stepped function in fig. 1 numbers of gust cycles for the flights A - K were obtained as shown in table 5.

The sequence of the gust cycles in the flights is one of the variables to be studied in the present program, that means a random sequence has to be compared with a programmed sequence. It should be noted that each positive gust amplitude is immediately followed by a negative one of equal magnitude. In other words gust cycles are applied as complete cycles around a mean load. This applies to both the random and the programmed sequence, see figure 3. For the random gust loads this is a restriction on the randomness, which is thought to be slightly conservative (ref. 3), see also the discussion in section 7.5.

The sequence of gust cycles of different magnitudes in each flight is a random sequence produced by a computer. An example is shown in fig. 2, see also fig. 3. The sequence of the flights is also random, with the exception of the very severe flights. Since it had to be expected that the severe flights may have a predominant effect on crack growth it was thought undesirable that these flights have a chance to cluster together, which is the risk of a random selection. The most severe flights were therefore uniformly distributed over the total sequence. This is diagrammatically indicated in table 6.

In the tests such a block of 5000 flights was repeated periodically. Since a block of 5000 flights contains approximately 200.000 gust cycles in a random sequence the repetition of the block is thought to be irrelevant with respect to the randomness of the load-time history. It was recommended in ref. 1 that the maximum load in a full-scale flight simulation test should not exceed the load level

anticipated 10 times in the desired life time in view of the predominant and favorable effect of larger loads on the fatigue life. If the desired fatigue life is taken as 50.000 flights this leads to a truncation at the load level that will be reached or exceeded once in 5000 flights, that means the maximum level shown in fig. 1.

A similar recommendation was made in ref. 1 for crack propagation. Assuming an inspection period of 500 flights the stress amplitude that is equalled or exceeded 10 times in 500 flights (or 100 times in 5000 flights) according to fig. 1 is about 6.6 kg/mm^2. This truncation level was used in several test series, but in addition two higher truncation levels (S_a = 7.7 and 8.8 kg/mm^2) and two lower ones (S_a = 5.5 and 4.4 kg/mm^2) were employed. The test results clearly confirmed the slower crack propagation at higher truncation levels. A few preliminary tests were carried out with the load spectrum shown in fig. 1 fully untruncated.

5.2 The ground-to-air cycles and the taxiing loads.

In the preliminary tests the mean stress of the ground-to-air cycles (GTAC) was more or less arbitrarily assessed at S_m = 0. On this mean stress 20 taxiing loads cycles were superimposed with an amplitude of S_a = 1.4kg/mm^2, the stress range 2.8 kg/mm^2 thus being 40 °/o of the S_m-value of the gust cycles. A similar pattern for the taxiing loads was adopted previously by Grassner and Jacoby (ref. 6). It was considered to be a relatively severe air-ground-air transition, which was made somewhat more severe for the major part of the tests by adopting S_m = - 2.0 kg/mm^2 for the taxiing loads. Since it was expected that the damaging effect of the taxiing loads would be negligible (the tests have confirmed this view) it was thought unnecessary to refine the GTAC by varying both the number and the amplitude of these load cycles, although that would have been possible.

6 Test results.

6.1 Results of the flight-simulation tests.

In each specimen two cracks were started by the central notch. In general crack propagation was symmetric, that means $\ell_1 \approx \ell_2$, and hence all data presented will refer to the average crack length ℓ as defined in fig. 4. The complete crack propagation records for all specimens are presented in tables 7 and 8 by giving the incremental numbers of flights, Δn_i, corresponding to successive crack growth intervals, $\ell_i \rightarrow \ell_{i+1}$. The ℓ_i- values were associated to the scribe-line

markings on the specimens. The plotting positions for crack propagation curves have not been presented, but they can easily be calculated from the tables. An example with two crack propagation curves is given in fig.7.

The crack growth data were converted into crack propagation rates by taking at $\ell = (\ell_i + \ell_{i+1})/2$:

$$\frac{\Delta \ell}{\Delta n} = \frac{\ell_{i+1} - \ell_i}{\Delta n_i} .$$

This formula in fact gives the average crack rate of the crack growth interval, which is assumed to apply to midpoint of the interval, a sufficient approximation for small intervals. Calculations of the crack rate were made only for the mean result of each test series. The results have been plotted in figs 8-11.

The crack propagation life is defined as the number of flights for crack growth from $\ell = 10$ mm until complete failure. The crack propagation life turned out to be useful for a first appreciation of the trends emerging from the tests. Results are given in tables 11-17 and figs 13 and 14, which will be used as a starting point for the discussion. For a more refined approach the crack propagation data will be used.

6.2 Results of the constant amplitude tests and damage calculations.

The evaluation of the data was performed in a similar way as for the flight-simulation tests, see table 9. In fig.15 the results have been plotted as S-N data. Damage calculations could not be made for all tests since insufficient S-N data were obtained. However, it was possible to calculate the $\Sigma n/N$ value for the random tests (2024 specimens) with the GTAC being omitted (series No.45). This has been done in table 18 and the result was $\Sigma n/N = 3.4$. A still higher value has to be expected for the 7075 specimens since the n-values are appr. half as large as for the 2024 specimens, see table 16, while the N-values are only one fourth appr. (see fig.15).

Secondly the constant-amplitude data for both materials obtained at $S_a = 1.1$ and 2.2 kg/mm^2 allowed a prediction on the difference between the crack propagation lives with and without small gust cycles. Adopting the symbols:
M = crack propagation life <u>with</u> small gust cycles included, and
M'= crack propagation life <u>without</u> small gust cycles being applied, then the Palmgren-Miner rule for a test with the small gust cycles included can be written as:

$$\frac{M}{M'} + M.\left(\Sigma \frac{n}{N} \text{ for the small gust cycles per flight}\right) = 1 .$$

With this equation M' may be derived from M or vice versa. In the former case M' becomes infinite for many test series since the damage of the small gust cycles (second term in the equation) is already equalling or exceeding 1. This clearly illustrates that the Palmgren-Miner rule is highly overestimating the damage contribution of the small gust cycles. The same trend is observed when deriving M from M', that means calculating the reduced fatigue life when small gust cycles are included. The results are shown in table 19 and a comparison is made with the test results. The table shows that the prediction of the reduced fatigue life is much smaller than the reduced test life, again implying an overestimation of the damage contribution of the small gust cycles. This feature is also thought responsible for the high $\Sigma n/N$ obtained in the random tests without GTAC (table 18).

It is noteworthy that the overestimation of the damage contribution of the small gust cycles appears to be larger for the 7075 specimens than for the 2024 specimens, compare the ratios in the last column of table 19.

6.3 Results of the tests on the specimens with a central hole.

These tests were carried out on 2024 specimens only. The crack propagation records are given in table 10, while the average crack propagation curves are shown in figure 16. Crack nucleation occurs at the edge of the hole and the nucleation period was arbitrarily defined as the number of flights to create a crack with a length of 2 mm (ℓ' = 2 mm or ℓ = 12 mm, see fig.16). The crack propagation life then started and lasted until failure. The variable studied was the truncation level and fig.16 shows that this level had a large effect on the crack propagation life, similar to the results as found in the normal crack propagation tests, see table 14. However, for the crack-nucleation period the truncation effect is much smaller as clearly illustrated by the life ratios in fig.16.

In fig.17 the crack rates in the specimens with a central hole are compared with those of specimens with a small central notch. Comparative results were available only for $S_{a,max}$ = 6.6 kg/mm^2 (and $S_{a,min}$ = 2.2 kg/mm^2). The figure shows that after some crack growth the two curves practically coincide, as might be expected.

6.4 Some fractographic observations.

Although the 200 specimens tested would have allowed an extensive fractographic examination this was beyond the scope of the investigation. Some macroscopic observations will be recapitulated below, since they may have some meaning for explaining the trends of the crack propagation results. A few fractographs obtained with the electron microscope will be presented also.

A large number of specimens showed growing bands on the fracture surfaces, that could easily be detected by the unaided eye, see fig.18. The bands were better visible if the difference between the maximum and the minimum gust amplitude ($S_{a,max}$ - $S_{a,min}$) was large, while the bands were virtually absent when this difference was small. A similar correlation was found for the macroscopic roughness of the fracture surface, that means that the surface was relatively smooth for a high value of $S_{a,max}$ - $S_{a,min}$ and relatively rough if this difference was small. Both observations indicate that the interaction between high and low amplitude cycles had some effect on the cracking mechanism. Since fatigue striations could not be detected in the dark bands whereas they could be found between the dark bands the dash bands have to be associated with the load cycles with a high amplitude. The dark bands have been associated previously (ref.7) with some kind of a "brittle" crack extension. Since the bands were more clearly present for a high value of $S_{a,max}$ - $S_{a,min}$ the numerous low amplitude cycles apparently are conditioning the material in order to promote the brittle crack extension in the high amplitude cycles.

Macroscopically the fracture plane of a slowly propagating fatigue crack is perpendicular to the loading direction. When the crack propagation is accelerating the growing direction remains the same but the fracture plane will make an angle of 45 degrees with the loading direction. This transition from the "tensile" mode to the "shear" mode has frequently been observed and has been correlated with the transition from plane strain to plane stress conditions.

In the present investigation the transition was observed in all specimens, but this phenomenon in general did not develop as clearly as under constant-amplitude loading. This is probably a consequence of the variety of amplitudes applied. Low amplitudes will promote the tensile mode, whereas high amplitudes will promote the shear mode. These then are two competing influences and the result is a slow transition from one mode into the other one when the crack is growing.

Unfortunately the transition also occurred during the precracking of the 2024 specimens, while it has occurred to a minor degree in the 7075 specimens, see fig.18. Consequently the very first part of crack growth in the 2024 specimens may have been influenced by the retransition to the tensile mode. In order to check this point some test series were carried out on specimens precracked to a crack length $\ell = 6$ mm and $\ell = 5$ mm for the 2024 and the 7075 specimens respectively. As shown by plotting the crack rate as a function of the crack length in figs 8b and 8d a noticeable effect of the precracking was found only for the 2024 specimens truncated at a low $S_{a,max}$ value ($S_{a,max} = 4.4$ kg/mm^2) and this effect was restricted to the very first part of the crack growth. Therefore it will not be considered any further.

It is noteworthy that the macrobands were still visible after the transition from the tensile mode to the shear mode was completed, although it should be said that the bands were less distinct then.

Two stage carbon replicas for observation in the electron microscope were obtained from the fracture surfaces of several specimens, but as said before, a systematic study was not made. Striations could be observed in all specimens examined and two pictures are shown in fig.19. In general the striations were more clearly observed in the 7075 specimens than in the 2024 specimens, while several features were found that have been described elsewhere (recently in ref.8). If it had been possible to indicate the GTAC in the electron graphs this would have been a promising result. However, no conformation of this possibility was obtained for the random flight simulation tests. In the programmed flight simulation tests certain batches of gust cycles of equal magnitude could easily be indicated, see for instance the lower picture in fig.19. From this information the striations corresponding to the GTAC could be indicated in some cases, although in general this still remained difficult.

7 Analysis of the present results and comparison with data from the literature.

In the literature comparative investigations concerning macro-crack growth under flight simulation loading could hardly be found. This is somewhat surprising since the problem is an essential part of the fail-safe conception. However, the fatigue life of notched elements under flight simulation was studied in the literature and reference will be made to this work. Secondly some crack propagation studies under random loading without GTAC were also reported in the literature.

In this chapter the various aspects of the present investigation are discussed separately while a general discussion is given in the following chapter. Before the present results will be analysed the possibilities for interaction effects between load cycles of different magnitudes will be discussed first, since that may be helpful for explaining the empirical trends.

7.1 Interaction between load cycles of different magnitudes.

If the fatigue load is changed from one level to a second level (by either changing S_a or S_m or both) the fatigue crack propagation at the second level will initially be different from the propagation occurring when the second level had been applied from the beginning of the test. This interaction effect according to macroscopic observations was practically negligible if the change was an increase of the stress amplitude, whereas important crack growth delays were observed if the stress amplitude was reduced (refs 9 and 10). Positive peak loads could most drastically reduce the crack growth. The explanation was based on residual stresses set up in the crack tip region.

In recent publications of the group of McMillan, Pelloux and Herzberg (refs 11, 12 and 13) it has been suggested that crack tip blunting and sharpening as well as cyclic strain hardening may be of more than just secondary importance. This view was based on excellent electron fractography. In addition it appears that changes of the state of stress may also be significant. Low stress amplitudes are associated with slow crack propagation and plane strain at the tip of the crack (tensile mode fracture, macroscopically), while high stress amplitudes will induce fast crack propagation with predominantly plane stress at the tip of the crack (shear mode fracture). Changing from a low amplitude to a high amplitude may then imply that the crack front has not the spatial configuration associated with the high amplitude. The same applies to the reversed amplitude change and this phenomenon will also lead to interaction effects. It is partly confirmed by the fractographic observations presented in section 6.4

Listing the various arguments for interaction effects during crack propagation gives:

1. Residual stresses.
2. Crack blunting or sharpening.
3. Cyclic strain hardening (or softening) and associated influences on the material structure.
4. Mismatch between the macroscopic fracture planes as a consequence of different states of stress at the tip of the crack.

It has been known for a long time that crack growth at a certain stress amplitude is depending of the mean stress (or the maximum stress). This result is substantiated by physical conceptions about crack extension (refs 14 and 15). It is then a natural consequence that residual compressive stresses will reduce the crack propagation rate. It is much more difficult to make qualitative predictions on the effect of the other aspects listed above. Crack blunting is a matter of plastic deformations and it therefore will introduce residual stresses. Hence the effect of crack blunting cannot be separated from an additional effect of residual stresses. It is noteworthy, however, that the interaction effects are more significant for the 7075 alloy as compared to the 2024 alloy, see section 7.9. In the former alloy higher residual stresses can be introduced due to the higher yield stress, and secondly crack blunting will be less than in the more ductile 2024 alloy. The larger interactions in the 7075 alloy are then in favor of the residual stress argument rather than crack blunting.

The third and the fourth argument do not readily allow simple speculations. In section 6.4 it was said that low amplitude cycles may condition the material and thus stimulate brittle crack extension at a higher amplitude, which would be an unfavorable interaction.

It is noteworthy that McMillan and Pelloux (refs 11 and 12) on the basis of electron fractography came to the conclusion that interaction effects when changing the fatigue load are hardly observed on the fracture surface. An exception, however, was made for the first cycle applied after changing the fatigue load. There were some indications that interactions might be active then. It was further observed by McMillan and Herzberg (ref.13) that a drop of S_{max} first induced an increased striation spacing followed by a decreased spacing afterwards. The latter as well as the macroscopically delayed crack growth are compatible with the residual stress argument, whereas the former is not.

An important conclusion from the above discussion is that changing the fatigue load may introduce an interaction that is only significant for the first

cycle following that change. The implication is that interaction effects could be very important for random load sequences, since the amplitude is changing from cycle to cycle. However, for tests with a programmed load sequence such interaction effects may remain almost unnoticed since changing the stress amplitude is a relatively infrequent occurrence.

In conclusion it has to be admitted that with the exception of the influence of residual stresses the qualitative understanding of the other interaction effects is still partly speculative and requires a further systematic study.

7.2 The omission of the taxiing loads (TL) from the ground-to-air cycle (GTAC).

As shown by table 11 the omission of the TL had a practically negligible effect on the crack propagation life. Important arguments are:

(a) The minimum stress in the GTAC (S_{min}) was the same for tests with and without TL.

(b) S_{min} in the GTAC was the lowest stress of a flight.

(c) The TL had a compressive mean stress ($-$ 2.0 kg/mm^2).

In view of the last argument it is difficult to see how the TL should contribute to crack growth. In view of arguments (b) and (c) the omission of the TL does not affect the overall loading cycle of a flight. Hence one should expect a negligible effect on the crack propagation life as shown by the tests. This justifies the omission of TL in a flight simulation test, provided that the minimum stress of the GTAC has been adjusted in order to account for the largest taxiing load cycle. (a) The omission may save a considerable amount of testing time.

The same reasoning was already presented in ref.1 for full-scale testing in general. Reference was made there to results of Gassner and Jacoby (ref.6) who found that the omission of 20 TL cycles per GTAC did not affect the fatigue life in flight simulation tests on notched bars (K_t = 3.1) of 2024-T3 material.

7.3 The minimum stress of the GTAC.

The minimum stress (S_{min}) of the GTAC was in fact not a parameter to be studied in the present test series. However, since some exploratory tests were carried out at S_{min} = -1.4 kg/mm^2 while for other tests a value of -3.4 kg/mm^2 was adopted a limited comparison could be made. Table 12 shows that the effect of S_{min}

(a) If a part of a structure is carrying a significant tensile stress during the GTAC it will be clear that TL may give the major fatigue damage contribution and TL should obviously be considered.

for the 7075 specimens was negligible whereas for the 2024 specimens there might be a small systematic effect, that means a shorter crack propagation life if the GTAC is going further downwards. The latter trend has not been well substantiated in view of the small number of tests.

In the GTAC the specimens were loaded in compression and one may expect the crack to be closed and to be no longer a severe stress raiser, since it then can transmit compressive loads. As a consequence the effect of S_{min} should be unimportant. This argument was suggested by Illg and McEvily (ref.16) who found it to be more applicable to 7075 sheet material as compared to 2024 sheet material. The latter was explained by the higher ductility of the 2024 alloy, implying more crack opening due to plastic deformation in the crack tip area, and hence a larger compressive stress before crack closure occurs. This reasoning is in agreement with the effect of S_{min} in the GTAC as indicated above.

The meaning of S_{min} of the GTAC for notched elements will be more important than for macro-cracks, since the crack-closing argument does no longer apply. Hence the assessment of S_{min} in a full-scale test on a structure should be made most carefully, the more since there is ample evidence of the large damaging influence of the GTAC (refs 1 and 17).

7.4 Omission of the small gust loads.

Omission of the smaller gust load cycles implies that a relatively large part of the gust cycles is omitted (see table 5) and hence much shorter durations of the flights will be the result, see fig.3. Testing times for 5000 flights were:

All gust cycles included : 346 minutes
Gusts with S_a = 1.1 kg/mm^2 omitted : 96 minutes
Gusts with S_a = 1.1 and 2.2 kg/mm^2 omitted : 30 minutes.

The attractive feature of omitting the smaller gust cycles is thus clearly illustrated. However, the omission in general increased the crack propagation life, see table 13 and fig.13. If the cycles with both S_a = 1.1 and S_a = 2.2 kg/mm^2 were omitted the increase of life was about twofold, for both random and programmed flight simulation tests and for two truncation levels ($S_{a,max}$ = 6.6 and 7.7 kg/mm^2). When omitting only the smallest cycles (S_a = 1.1 kg/mm^2) the increase was about 20 % for the 2024 specimens and 40 % for the 7075 specimens (table 13). The former result is a moderate increase and it might be acceptable under certain circumstances.

The effect of omitting small gust loads is shown in more detail in fig.9 by plotting the crack rate as a function of the crack length. It turns out that the larger differences are found if the crack rate is low while for relatively large cracks and high crack rates the effect has vanished. The trend is more clear for the 7075 alloy.

For an explanation two lines of thoughts may be considered:

(a) During the small gust cycles there will be some crack extension. In other words these cycles give some direct contribution to the crack propagation.

(b) Secondly the small gust cycles may induce an unfavorable interaction effect on the crack extension during larger amplitude cycles, see the discussion in section 7.1.

The fractographic observations (section 6.4) seem to favor the latter view, since the macro growth bands were more readily visible if the small gust cycles were included. However, as pointed out in section 7.1 it remains difficult to separate the contributions of the possibilities (a) and (b).

Comparable evidence was not found in the literature. Tests of McMillan and Pelloux (ref.11) with programmed sequences (without GTAC and not conforming to a gust spectrum) indicate little if any damage of the low amplitude cycles, but these cycles were so less numerous that a comparison with the present data is hardly justified.

Flight simulation tests on notched elements, involving the effect of omitting small gust cycles were reported by Naumann (ref.3) and by Gassner and Jacoby (ref.6). Naumann employing random flight-simulation loading found a small life increase when omitting gust cycles with $S_a = 1.05$ kg/mm^2, namely 16 and 7 per cent depending of S_{min} in the GTAC (7075 edge notched specimens, $K_t = 4.0$, S_m = 14 kg/mm^2). Gassner and Jacoby reported a 2.5 times longer fatigue life in programmed flight simulation tests if the cycles with the smallest amplitude ($S_a = 1.3$ kg/mm^2) were omitted (2024 central-notch specimens, $K_t = 3.1$, $S_m = 9.5$ kg/mm^2).

7.5 The effect of the gust cycles with a high amplitude.

The truncation of the gust spectrum (see fig.1), implies that the amplitude of the more severe gust cycles are reduced to a common $S_{a,max}$-value. The present results have shown that this value has a predominant effect on the crack propagation life, see table 14 and fig. 14. The latter figure clearly illustrates that the effect is large, irrespective of random or programmed gust sequences being adopted and taxiing loads being applied or not. Table 14 further shows that the effect is of a similar magnitude if the two smallest gust cycles are omitted ($S_{a,min}$ = 3.3 kg/mm^2). Figure 14 also shows that the effect is slightly larger for the 7075 alloy than for the 2024 material.

The effect of the truncation level is shown in more detail in fig. 8. The figures 8a and 8b indicate that the effect for the 7075 material has a maximum at $\ell \approx 20$ mm, whereas such a maximum is less clear for the 2024 specimens. Figure 8e including some data for $S_{a,max}$ = 12.1 kg/mm^2 most dramatically demonstrates the significance of truncating the gust spectrum. A test with $S_{a,max}$ = 12.1 kg/mm^2 on a 2024 specimen had to be stopped in view of the extremely slow crack growth.

For an explanation the interaction effects mentioned in section 7.1 have to be considered. Since the trends were the same for programmed and random gust sequences and also for random sequences with and without small gust cycles it is thought that residual stresses were indeed the main agent responsible for the effect of the truncation level.

In view of the predominant and almost frightening effect of $S_{a,max}$ on the crack propagation a few tests were carried out to explore this effect with regard to the life time for crack nucleation from a central hole. These tests were restricted to 2024 specimens and as fig. 16 shows the effect fortunately is much smaller for the nucleation period. It has to be admitted, however, that for the nucleation period the truncation levels were relatively low when considering for instance a target life of 50000 flights. More tests on this topic with respect to the pre-crack life appear to be desirable.

In the literature similar tests concerning crack propagation were not found and there was only one reference for the fatigue life under flight simulation loading for notched elements. Gassner and Jacoby (ref.6) for a notched bar (2024-T3, K_t = 3.1, S_m = 9.5 and 11.0 kg/mm^2) with programmed flight simulation loading reported as 30 and 10 percent life reduction when $S_{a,max}$ was reduced from 2.1 S_m to 1.55 S_m. Qualitatively it is the same trend as in the present investigation.

7.6 Random or programmed sequences in each flight and reversion of the gust cycle.

Within a flight the gusts were applied in either a random or a programmed sequence see fig.3. As table 15 shows the differences between the crack propagation lives for the two sequences were very small. This is further substantiated by fig.11. Table 15 gives the impression that the truncation level might have a small systematic effect on the comparison that means that for $S_{a,max}$ = 8.8 kg/mm^2 the crack propagation life with a programmed gust sequence is some 10 percent longer than for the random sequence, while for $S_{a,max}$ = 4.4 kg/mm^2 it is about 7 percent shorter. However, these differences are so small that it cannot be said with any certainty that a systematic trend was found.

In two test series the reversion of the gust cycles (random sequence) implied that each gust cycle now started with the negative half cycle followed by the positive one of the same amplitude. It turned out that the effect on the crack propagation was practically negligible, see table 15 and fig.10. This is a second indication that the sequence of the gust loads in a flight is of secondary importance. Apparently the $S_{a,max}$-value, within the limits of flight-simulation loading, was the predominant parameter for crack propagation rather than the load sequence in each flight.

Crack propagation under random loading, however, without GTAC but axial loading and positive mean stresses was studied by Smith (refs 18 and 19) for 2024 and 7075 sheet material and for different shapes of the spectral density function of the loading. The results indicated a small influence of the spectral shape. A similar trend was observed for the fatigue life of notched aluminum alloys by Kowalewski (ref.20, K_t = 1.8, plane bending, S_m = 0), Naumann (ref.21, K_t = 4, axial loading, S_m = 12.2 kg/mm^2) and Clevenson and Steiner (ref.22, K_t = 2.2, axial loading, S_m = 0). Since the "degree" of randomness is a function of the spectral shape those test programs suggest the sequence of loads to be of minor importance as long as it is random (see also the discussion of Swanson in ref.23). If periodic loads such as the GTAC are then added to a random load history it may be expected that the sequence effect will be limited even further.

Interesting information is coming from random tests published by Naumann (ref.3) and Gassner and Jacoby (ref.24). Naumann performed tests on an edge notched specimen ($K_t = 4$) of 7075 material with a random gust loading with and without GTAC. Three types of randomness were adopted, indicated by Naumann as:

(1) Random cycle: Each positive half cycle was followed by a negative half cycle of the same magnitude.

(2) Random half cycle, restrained: Each positive half cycle was followed by a negative half cycle, the magnitude of which was selected at random from the load spectrum and which therefore was generally not equal to that of the preceding positive half cycle.

(3) Random half cycle, unrestrained: Positive and negative half cycles were randomly selected with no restrictions on the sequence of positive and negative.

The results are summarized in the table below.

Randomness	Fatigue life in flights		Fatigue life ratio[a]	
	No GTAC	GTAC	No GTAC	GTAC
(1) Random cycle	5815	1334	0.66	0.84
(2) Random half cycle, restrained	7358	1515	0.84	0.95
(3) Random half cycle, unrestrained	8798	1588	1	1

(a) Ratio = 1 for case (3)

Gassner and Jacoby (ref.24) performed flight simulation tests with a random gust sequence and with two different programmed sequences. The tests on 2024-T3 specimens ($K_t = 3.1$) yielded fatigue lives of 2500, 2800 and 5800 flights respectively. There were approximately 400 gust cycles per flight programmed in a high-low-high amplitude sequence (life = 2800 flights) or in a low-high-low sequence (5800 flights). With such a large number of gust cycles per flight different programming techniques apparently may cause significantly different fatigue lives. Hence a realistic sequence should be preferred. In an additional study (ref.25) Jacoby performed flight simulation tests on the same specimen loaded with a random sequence of complete gust cycles,or with a random sequence of maxima and minima. The fatigue lives were practically the same. Jacoby also performed tests without GTAC and then found large differences between the fatigue lives under random and programmed load sequences, that means much larger as found in other investigations. The latter result requires further clarification and a discussion is beyond the scope of the present report.

7.7 Application of a single gust load per flight.

In the load sequence as shown in fig.3f, only the largest upward gust of each flight was applied. As a result the crack propagation life was more than 3 times longer as compared to the standard random sequence, see table 16. In fact such a highly simplified load sequence can be envisaged as a simulation of flights from which all gust cycles were omitted except for the positive half cycle with the largest amplitude. The fatigue life is longer than for omitting gust cycles with S_a = 1.1 and 2.2 kg/mm^2 as shown by table 16. The effect on the crack rate is illustrated by figs 8c and 8g. Apparently the simplification of applying a simple gust load per flight is unacceptable for crack propagation studies.

7.8 Omission of the GTAC.

Omission of the GTAC increased the fatigue life with some 50 and 80 percent for the 7075 and 2024 specimens respectively, see the bottom line of table 16. That means adding the GTAC reduced the fatigue life with 33 and 44 percent respectively. Hence the omission seems to be unjustified. The larger figure for the 2024 alloy may be explained in a similar way as the influence of S_{min} of the GTAC, see section 7.2.

In a previous investigation of this laboratory (ref.26) crack propagation in 2024 and 7075 sheet material under random and programmed load sequences was studied in an indoor and an outdoor environment. Data on the effect of the GTAC were available for the 2024 material only. The GTAC induced life reductions of 27 and 2 percent for the indoor and the outdoor environment respectively. The small reductions are not surprising when taking notice of the stress levels (kg/mm^2): gusts: S_m = 12.1, $S_{a,max}$ = 11.6, $S_{a,min}$ = 1.15, GTAC: S_{min} = + 2.6.

In another test series on 2024-T3 Alclad specimens (ref.27) a constant-amplitude loading (S_m = 9 and S_a = 3 kg/mm^2) was interspersed with GTAC (S_{min} = + 0.7 kg/mm^2) every 50 or every 10 cycles. Reductions of the crack propagation life were 12 and 28 percent respectively.

Much larger reductions have been found in several flight-simulation test series for notched specimens and structures (see for a survey Appendix G of ref.1) and hence realistic fatigue information requires a flight by flight testing. Although the present data have shown a smaller effect during macro-crack propagation it has to be said that a flight-simulation loading should be preferred also then rather than testing without GTAC or testing with ground-to-air cycles applied in groups.

7.9 Comparison between the two alloys, 7075 and 2024.

In general all tests were carried out on specimens of both alloys using the same stress-time histories. Without any exception the crack propagation life was larger for the 2024 alloys, and as shown by table 17 approximately twice as large. It was already illustrated by fig.14 that this ratio was dependent of the $S_{a,max}$-value, the ratio becoming smaller at higher truncation levels. In this respect it is interesting to compare the crack rates as a function of the crack length, see figures 10 to 12. This shows that the differences between the two alloys become smaller at higher values of the crack length (higher stress intensities), larger values of $S_{a,max}$ and smaller values of $S_{a,min}$. Apparently these trends indicate that favorable interaction effects become more significant in the 7075 material as compared to the more ductile 2024 alloy if the stress intensity at the tip of the crack is increased (higher ℓ and $S_{a,max}$). This argument was referred to in section 7.1.

It is noteworthy that the differences between the two alloys were considerably larger in the constant-amplitude tests, see fig.15, than in the flight-simulation tests. This is another indication for the more favorable interaction effects in the 7075 alloy.

7.10 Damage calculations.

It was shown in section 6.2 that $\Sigma\, n/N = 1$ highly underestimates the crack propagation life for the tests without GTAC. Calculations for tests with GTAC could not be made since constant-amplitude data for the GTAC were lacking.

A comparison between predicted crack rates and actual crack rates under random loading conditions (without GTAC) was made by several authors. For a positive mean stress Smith (ref.18) found the linear damage rule to be conservative (2024 and 7075 material) while Swanson et al (ref.28) arrived at good estimates (7079 alloy). Both investigations apply to axial load tests. For program loading $\Sigma\, n/N$ far in excess of one had previously been found (ref.29).

As shown by table 18 the damage contribution in the flight-simulation tests should be very small for the higher S_a-values. However, according to the test results, load cycles with the high S_a-values had a large positive effect on the crack propagation life, rather than a small negative one.

It was already mentioned in section 6.2 that the Palmgren Miner rule also gave a very bad prediction of the damage of the small gust cycles (table 19). The invalidity of the Palmgren Miner rule is not a surprising conclusion since interaction effects as discussed in section 7.1 are essentially ignored by this rule. However, from the present data the conclusion can also be given as follows:
The effect of changing the load spectrum on the fatigue life cannot be predicted from the Palmgren Miner rule.

8 Discussion.

8.1 Recommendation for the maximum load in a flight-simulation test.

The main theme of the present investigation is the question: Which load sequences can be adopted in a flight simulation test in order to obtain crack propagation data with practical significance? This is an urgent question if fail-safe tests are carried out on a full-scale structure. It appears that the present investigation has shown some variables to be of minor importance and some others to be of major importance.

1. The omission of taxiing loads did not affect the crack propagation.
2. The minimum stress in the GTAC, being compressive, had only a small influence if any.
3. The sequence of the gust cycles in a flight turned out to be of secondary importance.

Influences of major importance were concerned with the following topics:

4. Omission of the gust cycles with small amplitudes did systematically increase the fatigue life, see fig.13, and should therefore be limited to very small amplitudes (say $S_a \leq 1$ kg/mm^2).
5. The predominant effect on the crack propagation was exerted by the maximum gust amplitude ($S_{a,max}$) included in the test, see fig.14. Increasing this amplitude gave a considerable decrease of the crack propagation rate.

In fact the selection of $S_{a,max}$ now appears to be the most delicate issue when planning a flight-simulation program for crack propagation studies. Although it may appear realistic to apply all gust loads that are anticipated to occur, it has to be recognized that one then applies an averaged expected load spectrum. The load spectrum is statistically variable in such a way that the spectrum for a certain aircraft will be more severe, while it will be less severe for another nominally identical aircraft. If the target for the crack propagation life is

2000 flying hours (as an example) the gust load that on the average is reached or exceeded once in that period will be met more than once by some aircraft while others will not see it. If we then know that this high gust load is highly beneficial for a slow crack propagation it would be both unrealistic and unconservative to include it in a test. A truncation of the load spectrum to a lower level has therefore to be proposed.

In ref.1 a similar argumentation was already used for full-scale testing in general and it was proposed that a load level exceeded 10 times in the target life should be the maximum level applied in the test. The number of 10 admittedly has been chosen somewhat arbitrary, but the number is thought to be large enough for being sure that each aircraft will meet the load at least a few times. The recommendation presupposes that the load spectrum was estimated as accurately as possible without any unduly over-conservatism.

It now appears that the same recommendation is equally applicable to crack propagation studies. The question then arrises as what shall be the target life for crack propagation. For a fail-safe structure the target may obviously be much lower than the anticipated useful life of the aircraft. It has to be associated with the inspection period in service. The proposal is to truncate the load spectrum at the level that will be equalled or exceeded 10 times in the service inspection period. The question of safety factors is again difficult and will not be discussed here. It should be pointed out, however, that the truncation as suggested is in some way accounting for the scatter of the load spectrum.

8.2 Alternatives to flight-simulation.

For full-scale fatigue testing only one structure will in general be available and there appears to be no reasonable alternative to a realistic flight-simulation test. This view has been expressed several times, notably by Branger (ref.30). It appears to be true also for crack propagation. Fortunately the problems of load control in such a test are no longer an objection.

If smaller structural elements have to be tested during the design stage it may be worthwhile to adopt simpler testing methods such as program tests or even constant-amplitude tests. For crack propagation there appears to be as yet no empirical justification for such a procedure. On the contrary the present investigation suggests that interaction effects between load cycles of different amplitudes are important enough to retrieve the main line of service loading. This is the

flight-by-flight character, at least for a wing structure mainly loaded by gusts. In other words also then a flight-simulation test has to be advocated. As discussed by Jacoby (ref.25) this is no longer a problem for modern fatigue machines. A major difficulty, however, is to arrive at a useful flight-simulation load-time history.

If one still uses simpler loading programs in view of available fatigue apparatus one has to consider the uncertainties regarding the relevance of the test results.

Finally an alternative solution might be "calculations", or borrowing and extrapolating from data in the literature. It is almost euphemistic to state that this problem has not yet been solved. Nevertheless there are certain prospects for the future. A discussion would be beyond the scope of this report.

8.3 Suggestions for further work.

1. An obvious recommendation is to perform a similar test program as the present one, but now with typical notched elements as a specimen in order to cover the fatigue life part of the problem. Although some studies were reported in the literature as referred to in the previous chapter (see also the exploratory tests of the present investigation, fig.16) several aspects have to be studied in more detail.
2. Regarding crack propagation in aluminum alloys systematic studies of interaction effects are certainly worthwhile. In other words the accumulation of fatigue damage is still a topic of present interest, both for practical and fundamental reasons.
3. Fatigue under random loads generally appears to be a useful field for investigations. This topic was extensively reviewed by Swanson (ref.23) and the recommendations at the end of his recent paper are well taken.
4. A study of the characteristics of flight-simulation loading should be recommended. The application of such load histories in fatigue tests for various purposes has to be considered. One aspect of this problem is the mixture of random and non-random loads.

9 Conclusions.

Flight-simulation tests with various load sequences were carried out to study the macro-crack propagation in sheet specimens of 7075-T6 and 2024-T3 clad material. A gust load spectrum was adopted, the mean stress being 7.0 kg/mm^2 (10 ksi). In each test 10 different types of flight were simulated varying from good to bad weather conditions. A variety of load sequences has been adopted related to the truncation of high-amplitude gust cycles, to the omission of low-amplitude gust cycles, taxiing loads and ground to air cycles, and to random and programmed gust sequences in a flight (see figs 1 and 3 and table 1). About 200 specimens were tested. The main results of the investigation are summarized in the conclusions below.

1. Omission of the taxiing loads from the ground-to-air cycles did not affect the crack propagation.
2. In the majority of tests S_{min} of the ground to air cycle was -3.4 kg/mm^2 (4.8 ksi) but in a few exploratory tests a value of -1.4 kg/mm^2 (2.0 ksi) was used. The limited data indicated a practically negligible effect on the crack propagation.
3. Omission of the gust cycles with S_a = 1.1 kg/mm^2 (75 percent of the cycles) increased the crack propagation life with 20 and 40 percent for the 7075 and 2024 material respectively. Omitting the gust cycles with S_a = 1.1 and 2.2 kg/mm^2 (95 percent of the cycles) increased the life with some 100 percent (fig.13).
4. The predominant effect on the crack propagation life was exerted by the maximum amplitude of the gust cycles (truncation level). Increasing this amplitude from 4.4 to 8.8 kg/mm^2 (6.3 ksi to 12.6 ksi) linearly increased the crack propagation life from 2500 to 15000 flights and from 6000 to 25000 flights for the 7075 and 2024 specimens respectively (fig.14). The effect was somewhat larger for the 7075 alloy.
5. A programming of the gust cycles in each flight in a low-high-low sequence has given the same crack propagation as for the random sequence.
6. In the majority of tests complete gust cycles were applied, starting with the positive gust followed by the negative one of equal amplitude. Reversion of this sequence in negative-positive did not noticeably affect the crack propagation.
7. Application in each flight of the largest upward gust load only increased the crack propagation life approximately three times.
8. Omission of the ground-to-air cycle increased the crack propagation life approximately 1.5 and 1.8 times for the 7075 and the 2024 specimens respectively. This effect is smaller than usual for the fatigue life of notched elements.

9. The crack propagation life in the flight-simulation tests for the 2024 specimens were on the average twice as long as for the 7075 specimens. The ratio in some additional constant-amplitude tests was larger, namely approximately four.

10. Damage calculations have shown that the Palmgren-Miner rule highly misjudges the effect of changing the load spectrum both in the high-amplitude and in the low-amplitude region.

11. In some exploratory tests on specimens notched by a central hole the effect of truncating the high-amplitude gust cycles was smaller for the crack-nucleation period (up to crack length 2 mm) as compared to the large effect on the subsequent macro-crack propagation (fig.16).

12. A discussion on interaction effects between load cycles of different magnitudes indicates residual stresses, crack blunting, (cyclic) strain-hardening effects and mismatch between macro-fracture planes as the possible mechanisms for an explanation. It is thought that for the present test series residual stresses had a predominant effect with respect to the trends observed.

13. Conclusions 1-8 have some bearing upon proceduresfor full-scale tests conducted for obtaining crack propagation data in view of fail-safe considerations. With respect to the maximum load in such a test it has to be recommended that this load should not exceed the level which is anticipated to be equalled or exceeded ten times in the related inspection period.

10 List of references.

1. Schijve, J., Broek, D., deRijk, P., Nederveen, A. and Sevenhuysen, P.J. — Fatigue tests with random and programmed load sequences with and without ground-to-air cycles. A comparative study on full-scale wing center sections. NLR Report S.613, Amsterdam, Dec. 1965. Also AFFDL-TR-66-143, Oct. 1966.

2. Buxbaum, O., Gassner, E. — Häufigkeitsverteilungen als Bestandteil der Lastannahmen für Verkehrsflugzeuge. Luftfahrttechnik-Raumfahrttechnik, Vol.13, p.78, 1967.

3. Naumann, C.A. — Evaluation of the influence of load randomization and of ground-to-air cycles on fatigue life. NASA TN D-1584, Oct. 1964.

4. Bullen, N.I. — The chance of a rough flight. Royal Aircraft Establishment, TR No. 65039, February 1965.

5. Hoblit, F.H., Paul, N., Shelton, J.D. and Asford, F.E. — Development of a power-spectral gust design procedure for civil aircraft. FAA Techn. Report ADS-53, Jan. 1966.

6. Gassner, E., Jacoby, G. — Betriebsfestigkeitsversuche zur Ermittlung zulässiger Entwurfsspannungen für die Flügelunterseite eines Transportflugzeuges. Luftfahrttechnik-Raumfahrttechnik, Vol. 10, p. 6, 1964.

7. Proceedings of the Crack Propagation Symposium, Vol. 1 and 2, Cranfield 1961.

8. Broek, D. Van der Vet, W.J. — Systematic electron fractography of fatigue in aluminium alloys. NLR TR 68002, Nov. 1967.

9. Schijve, J. — Fatigue crack propagation in light alloy sheet material and structures.
Advances in Aeronautical Sciences, Vol. 3, p. 387. Pergamon Press, 1961.

10. Hudson, C.M. and Hardrath, H.F. — Investigation of the effects of variable-amplitude loadings on fatigue crack propagation patterns.
NASA TN D-1803, Aug. 1963.

11. Mc Millan, J.C. Pelloux, R.M.N. — Fatigue crack propagation under program and random loads. Fatigue Crack Propagation, ASTM STP 415, p. 505. Am.Soc.Testing Mats., 1967.

12. Mc Millan, J.C. Pelloux, R.M.N. — Fatigue crack propagation under programmed and random loads. Boeing Scientific Research Laboratories, Doc. D1-82-0558, July 1966.

13. Mc Millan, J.C. Hertzberg, R.W. — The application of electron fractography to fatigue studies. ASTM Paper No. 42, 70th Annual Meeting ASTM, Boston, June 1967.

14. Schijve, J. — Analysis of the fatigue phenomenon in aluminium alloys.
NLR TR M.2122, July 1964.

15. Schijve, J. — Significance of fatigue cracks in micro-range and macro-range. Fatigue Crack Propagation, ASTM STP 415, p. 415. Am.Soc.Testing Mats., 1967.

16. Illg, W. Mc Evily, A.J. — The rate of fatigue crack propagation for two aluminum alloys under completely reversed loading.
NASA TN. D-52, 1959.

17. Jacoby, G. — Comparison for fatigue life estimation processes for irregularly varying loads.
Proc. 3rd Conference on Dimensioning and Strength Calculations, Hungarean Academy of Sciences, p.81, Budapest 1968.

18. Smith, S.H. — Fatigue crack growth under axial narrow and broad band random loading. Paper in: Acoustical Fatigue in Aerospace Structures, (ed. by W.J. Trapp and D.M. Forney Jr.), p.331. Syracuse Un.Press, 1965.

19. Smith, S.H. — Random-loading fatigue crack growth behavior of some aluminium and titanium alloys. Structural Fatigue in Aircraft, ASTM STP 404. P.76 Am.Soc. Testing Mats., 1966.

20. Kowalewski, J. — On the relation between fatigue lives under random loading and under corresponding program loading. Full-Scale Fatigue T esting of Aircraft Structures (ed. by F.J. Plantema and J. Schijve), p. 60, Pergamon Press, 1961.

21. Naumann, E.C. — Fatigue under random and programmed loads. NASA TN D-2629, Febr. 1965.

22. Clevenson, S.A., Steiner, R. — Fatigue life under random loading for several power spectral shapes. NASA TR R-266, Sept. 1967.

23. Swanson, S.R. — Random load fatigue testing: A state of the art survey. Materials Research and Standards, Vol. 8, No. 4, p.11, April 1968.

24. Gassner, E., Jacoby, G. — Experimentelle und Rechnerische Lebensdauer-beurteilung von Bauteilen mit Start-Lande-Last-wechsel. Luftfahrttechnik-Raumfahrttechnik, Vol. 11, p.138, 1965.

25. Jacoby, G. — Comparison of fatigue lives under conventional program loading and digital random loading. Paper presented at the ASTM Fall Meeting, Atlanta, 29 Sep. - 4 Oct. 1968.

26. Schijve, J., de Rijk, P. — The crack propagation in two aluminium alloys in an indoors and an outdoors environment under random and programmed load sequences. NLR-TR M. 2156, Nov. 1965.

27. Schijve, J., de Rijk, P. The effect of ground-to-air cycles on the fatigue crack propagation in 2024-T3 Alclad sheet material. NLR Report M.2148, July 1965.

28. Swanson, S.R., Cicci, F. Hoppe, W. Crack propagation in clad 7079-T6 aluminum alloy sheet under constant and random amplitude fatigue loading. Fatigue Crack Propagation, ASTM STP 415, p. 312. Am.Soc.Testing Mats., 1967.

29. Schijve, J. and Broek, D. Crack propagation. The results of a test programme based on a gust spectrum with variable amplitude loading. Aircraft Engineering, Vol. 34, p. 314, 1962. Also NLR MP.208, Dec. 1961.

30. Branger, J. The full-scale fatigue test on the DH-112 Venom AC carried out on the fatigue history simulator by F and W, Emmen. Eidg. Flugzeugwerk Emmen, Bericht S-163, 1964.

Table 1 Survey of the test parameters in the various test series.

Stresses in kg/mm^2 , 1 kg/mm^2 = 1.422 ksi

Gust cycles: S_m = 7.0 kg/mm^2

Taxiing loads: S_{max} - S_{min} = 2.8 kg/mm^2 , 20 cycles per GTAC.

Load sequence	GTAC		Gust loads		Test series No. (a)	
	S_{min}	Taxiing loads	$S_{a,max}$	$S_{a,min}$	7075-T6	2024-T3
Random (exploratory tests)	-1.4	yes	12.1	1.1	1 (1)	2 (1)
			7.7		3 (1)	
			6.6		4 (1)	7 (1)
			5.5		5 (1)	
			4.4		6 (1)	8 (2)
Random	-3.4	yes	8.8	1.1	9 (1)	
			7.7		10 (5)	21 (1)
			6.6		11 (5)	22 (5)
			7.7	3.3		23 (1)
			6.6		12 (4)	24 (4)
		no	8.8	1.1	13 (4)	25 (4)
					13a (2)	25a (2)
			7.7		14 (4)	26 (5)
			6.6		15 (6)	27 (4)
					15a (2)	27a (2)
			5.5		16 (4)	28 (4)
			4.4		17 (4)	29 (4)
					17a (4)	29a (2)
			6.6	2.2	18 (4)	30 (4)
			7.7	3.3	19 (2)	31 (3)
			6.6		20 (4)	32 (4)
			1 gust load per flight (b)		46 (4)	47 (4)
	GTAC omitted		6.6	1.1	44 (4)	45 (4)
Random, reversed gusts	-3.4	no	6.6	1.1	42 (4)	43 (4)
Programmed	-3.4	yes	7.7	1.1	41 (1)	
		no	8.8	1.1	33 (4)	37 (4)
			6.6		34 (4)	38 (4)
			4.4		35 (4)	39 (4)
			6.6	3.3	36 (4)	40 (4)

(a) The numbers between brackets indicate the number of tests carried out.
(b) $S_{a,max}$ = 6.6

Table 2 Survey of the flight-simulation tests on sheet specimens with a central hole.

Specimen size: Length and width similar to crack propagation specimen, see fig.4. Central hole with diameter 20 mm.

Material: 2024-T3 Alclad.

Gust cycles: S_m = 7.0 kg/mm^2.

Stresses in kg/mm^2 , 1 kg/mm^2 = 1.422 ksi.

Load sequence	GTAC		Gust loads		Test series No. (a)
	S_{min}	Taxiing loads	$S_{a,max}$	$S_{a,min}$	
Random	-3.4	no	8.8 6.6 4.4	2.2	48 (4) 49 (4) 50 (4)

(a) The numbers between brackets indicate the number of tests carried out.

Table 3 Survey of the constant-amplitude tests

S_m = 7.0 kg/mm^2 , load frequency 10 cycles per second.

Material	S_a (kg/mm^2)	Specimen No.	Crack propagation life (kilocycles)
7075-T6	2.2 1.1	B19/B7 B80/B93 B6 /B13	31.3/32.0 192/181 (a)
2024	8.8 6.6 4.4 2.2 1.1	A61 A55 A54 A50/A105 A44 A7 /A57	2.65 8.63 21.2 124/125 1031 (b)

(a) Crack propagation started at $l \geqq 18$ mm } Specimens previously used for
(b) Crack propagation started at $l \geqq 14$ mm } flight-simulation tests.

Table 4 Static properties of the materials.

Material	Direction of loading	S_u (kg/mm^2)	S_u (ksi)	$S_{0.2}$ (kg/mm^2)	$S_{0.2}$ (ksi)	Elongation (2 in.gage length)
2024-T3 Alclad	Longitudinal	47.4	67.4	36.0	51.2	18 %
	Transverse	45.6	64.8	31.0	44.1	21 %
7075-T6 Clad	Longitudinal	53.9	76.6	48.5	69.0	13 %
	Transverse	54.1	76.9	47.2	67.1	13 %

All data in this table are mean values of six tests.

Table 5 Gust load occurrences in the 10 different types of flights

Flight type	Number of flights in 5000 flights	Number of gust cycles with amplitude S_a (kg/mm^2)											Total number of cycles per flight
		S_a=12.1	S_a=11.0	S_a=9.9	S_a=8.8	S_a=7.7	S_a=6.6	S_a=5.5	S_a=4.4	S_a=3.3	S_a=2.2	S_a=1.1	
A	1	1	0	1	1	2	3	5	9	15	27	43	107
B	2		1	1	1	1	2	4	8	14	26	43	101
C	2			1	1	1	2	3	7	12	25	43	95
D	10				1	1	1	3	5	11	24	43	89
E	27					1	1	2	3	9	22	43	81
F	91						1	1	3	7	18	43	73
G	301							1	2	4	15	42	64
H	858								1	3	11	38	53
J	3165									1	7	28	36
k	543										1	19	20
Total number of cycles in all flights		1	2	5	15	43	139	495	1903	8000	39252	149902	
Number of exceedings, see fig.1		1	3	8	23	66	205	700	2603	10603	49855	199757	

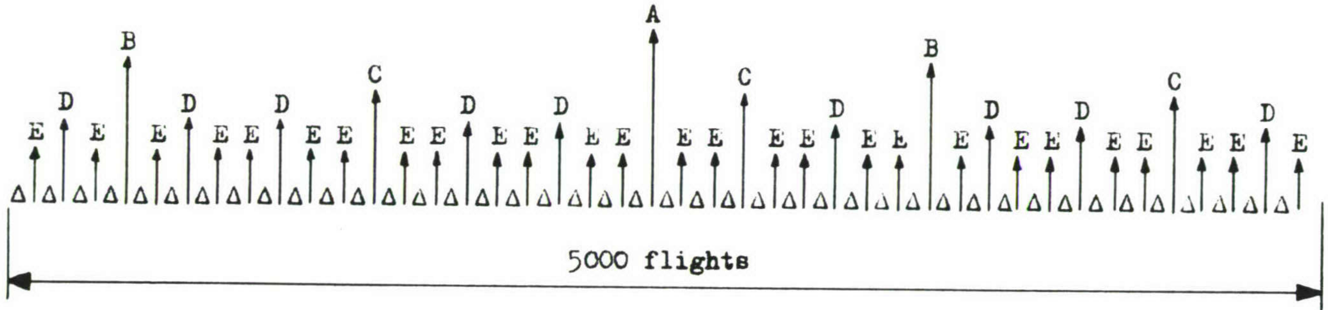

The most severe flights A, B, C, D, E, are shown separately.

These flights are homogeneously distributed over a sequence of 5000 flights.

Δ indicates a group of 118 flights.

The 42 groups Δ consist of a random sequence of:

91 flights type F
301 flights type G
858 flights type H
3165 flights type J
543 flights type K

<u>Table 6</u> <u>Diagrammatic picture of the sequence of the various flights in 5000 flights</u>

Table 7 Crack propagation records of the flight-simulation tests. Values of Δn in numbers of flights.

- First column: crack length interval.
- First and second line: Test series No. and Specimen No. A dash indicates that the two specimens were tested in series. Arithmetrical mean values of Δn are given in the last columns of the test series. The two bottom values in these columns are the arithmet ical and the geometrical mean values of the crack propagation lives (l = 10-80 mm).

$l_i - l_{i+1}$	3	4	5	6	7	8			9	10				
(mm)	B21	B90	B50	B41	A2	A47	A1	Mean	B2	B20/B89		B22/B71		Mean
10-12	584	668	407	366	1631	951	-	951	589	452	661	591	602	577
12-14	748	390	304	229	1999	848	-	848	764	642	652	566	725	646
14-16	668	392	301	208	1862	705	-	705	1027	735	688	657	717	699
16-18	708	359	223	176	1723	585	-	585	909	716	657	594	701	667
18-20	706	316	212	162	1496	517	783	650	973	818	781	658	785	761
20-25	1800	328	596	306	3270	989	1141	1065	3151	1805	1826	1718	1795	1795
25-30	1762	428	408	225	1892	883	786	835	2569	1568	1561	1572	1624	1581
30-35	1368	936	350	200	1390	455	524	480	1789	1106	1089	1177	1076	1112
35-40	947	302	223	184	675	271	319	295	1073	535	-	736	484	585
40-45	342	129	78	85	342	141	165	153	338	127	-	339	-	233
45-50	111	45	52	44		69	64	67	148	-	-	74	-	74
50-55	-	-	-	16	28	15	24	20	49	-	-	17	-	17
10-80	9617	4800	3075	2205	16308	6240	6793	6516 6511	13406	8568	8641	8716	8956	8720 8719

$l_i - l_{i+1}$	11						12					13				
(mm)	B67 /	B24	B42	B4/B53		Mean	B27/B76		B47/B96		Mean	B25/B60		B45/B94		Mean
10-12	1227	556	632	612	575	594	1444	1236	1787	1645	1578	819	548	912	588	717
12-14		571	606	587	700	616	1594	1580	1621	2962	1598	912	863	891	777	861
14-16	448	545	474	585	625	535	1332	1390	1448		1390	1064	1081	918	887	988
16-18	452	416	362	502	546	456	1005	1198	1269	1262	1184	1253	1282	1179	1051	1191
18-20	397	359	424	474	486	428	875	958	1052	1100	996	1167	1187	1275	1270	1225
20-25	1020	1113	911	1088	1253	1077	1440	1629	1358	1795	1556	3274	3345	3442	3028	3272
25-30	902	933	911	895	994	927	523	-	736	891	717	2570	2427	2959	2592	2637
30-35	834	750	785	701	631	600	370	-	400	404	391	-	1217	-	1655	1436
35-40	181	-	424	345	-	317	245	-	230	-	238	-	585	-	664	625
40-45	86	-	136	109	-	110	103	-	108	-	106	-	254	-	295	275
45-50	64	-	44	51	-	53	58	-	-	-	58	-	120	-	39	80
50-55	24	-	2	45	-	24	-	-	-	-	-	-	27	-	-	14
10-80	5637	5600	5809	6001	6437	5897 5889	9010	9311	10089	11182	9898 9863	13269	12943	14298	12915	13356 13329

$l_i - l_{i+1}$	14					15							16				
(mm)	B40/B69		B8/B77		Mean	B88/B39		B68/B15		B5/B54		Mean	B57/B28		B48/B91		Mean
10-12	611	733	657	552	640	514	625	650	470	1164	752	602	435	472	436	503	462
12-14	591	778	712	710	698	475	429	500	466		581	494	379	443	452	405	420
14-16	659	721	750	733	716	387	440	479	432	558	573	477	328	317	342	364	338
16-18	651	687	713	673	681	395	397	429	503	448	405	430	282	343	319	337	320
18-20	786	762	811	723	773	346	364	395	334	414	449	384	309	299	289	278	294
20-25	1994	2230	1985	1812	2005	863	950	900	874	1123	1115	971	587	627	624	621	615
25-30	1943	1825	1765	1634	1792	763	848	841	797	1027	877	859	466	751	825	887	509
30-35	1374	1351	1239	1210	1294	475	-	521	545	-	487	507	267				291
35-40	749	565	-	654	656	183	-	203	227	-	206	205	197	156	134	141	157
40-45	168	-	-	227	198	104	-	82	-	-	81	89	71	94	63	-	76
45-50	-	-	-	80	80	37	-	47	-	-	38	41	35	-	40	-	38
50-55	-	-	-	-	-	14	-	-	-	-	13	14	-	-	-	-	-
10-80	9583	10061	9624	9019	9572 9565	4555	4865	5047	4738	5685	5583	5079 5062	3390	3571	3541	3656	3540 3538

$l_i - l_{i+1}$	17					18					19			20				
(mm)	B30/B73		B10/B59		Mean	B43/B92		B29/B78		Mean	B51/B85		Mean	B72/B23		B3/B52		Mean
10-12	417	322	359	345	361	810	810	927	979	882	2406	2776	2591	1660	1628	2016	1945	1812
12-14	316	274	342	222	289	773	770	846	808	799	2048	2534	2309	1770	1802	1681	1608	1715
14-16	234	248	168	219	217	771	810	849	811	810	2418	2400	2409	1576	1121	1219	1418	1334
16-18	237	231	417	174	214	893	845	759	758	814	2247	2820	2534	1162	1055	1141	1239	1149
18-20	202	161		194	186	591	566	1880	2054	579	1765	1746	1756	902	925	991	936	939
20-25	402	392	413	299	377	1571	1278			1425	5200	4919	5060	1125	1455	1335	1605	1380
25-30	359	317	337	288	325	1020	917	675	1078	923	2774	2937	2856	807	773	675	749	751
30-35	151	184	-	193	176	371	554	405	-	443	940	-	940	254	381	310	218	291
35-40	128	121	-	133	127	203	323	159	-	228	370	-	370	185	211	219	-	205
40-45	-	66	-	65	66	-	112	89	-	101		-		85	92	131	-	103
45-50	-	40	-	21	31	-	34	34	-	34		-		-	-	43	-	43
50-55	-	8	-	9	9	-	-	14	-	14		-		-	-	9	-	9
10-80	2565	2369	2461	2165	2390 2385	7159	7029	6649	7200	7009 7006	20552	21826	21189 21179	9515	9532	9872	10214	9783 9779

$l_i - l_{i+1}$	21	22						23	24					25				
(mm)	A81	A24	A84/A43		A99/A4		Mean	A48	A63/A6		A22/A79		Mean	A12/A69		A35/A85		Mean
10-12	1790	1655	1466	1198	1267	1237	1365	3093	3117	3528	2916	3436	3249	1706	1663	2194	1881	1861
12-14	2150	1269	1450	1461	1357	1473	1402	4893	2801	3038	3132	3297	3063	3365	2993	3336	3727	3355
14-16	2004	1127	1234	1369	1402	1482	1323	3839	2300	2768	2817	2667	2638	3420	3444	2946	3804	3404
16-18	1848	1019	1211	1256	1108	1280	1175	3608	2117	2114	2255	2426	2228	3205	2858	2899	3383	3086
18-20	1548	950	906	1070	1023	1084	1007	3122	1792	2261	1871	1842	1942	2615	2541	2127	2430	2428
20-25	2829	1748	1940	2119	2073	2376	2051		3427	3805	3672	3797	3675	4573	4362	3980	4635	4388
25-30	1848	1233	1259	1406	1407	1453	1352		2070	-	2156	2233	2153	2838	2418	2407	-	2554
30-35	1067	816	784	852	802	-	814		1094	-	1005	-	1050	-	1474	1194	-	1334
35-40	502	367	361	-	404	-	377		319	-	383	-	351	-	657	613	-	635
40-45	216	193	141	-	181	-	172		145	-	158	-	152	-	170	} 311	-	170
45-50	} 110	37	33	-	-	-	35		43	-	35	-	39	-	84		-	84
50-55		-	-	-	-	-			-	-	-	-	-	-	-	14	-	14
10-80	15921	10427	10808	11189	11112	10860	10879 10876	31000	19236	21196	20405	21284	20530 20513	24126	22683	22034	24410	23313 23292

$l_i - l_{i+1}$	26					27					28				
(mm)	A11/A68		A34/A91		Mean	A78/A28		A5/A100		Mean	A31/A88		A8/A65		Mean
10-12	1896	1440	1599	1816	1688	1542	1404	1381	1665	1498	1177	1202	1201	1210	1198
12-14	2231	2306	1915	2267	2180	1352	1398	1549	1542	1460	973	1008	1053	977	1003
14-16	2170	2197	2010	2205	2146	1260	1391	1466	1403	1380	832	898	967	839	884
16-18	1785	1996	1873	1875	1882	1148	1227	1146	1216	1184	812	750	713	742	754
18-20	1601	1647	1487	1493	1557	955	1117	1197	1046	1079	687	684	670	639	670
20-25	3063	3311	2502	2725	2900	1968	2130	2151	2218	2116	1226	1271	1235	1236	1242
25-30	1874	1957	1670	1788	1822	1370	1482	1447	1445	1436	953	982	915	921	943
30-35	1137	1115	1081	-	1111	817	855	913	870	864	594	622	570	565	588
35-40	633	519	428	-	527	441	-	469	423	444	301	334	282	306	306
40-45	194	-	187	-	191	193	-	216	203	204	146	-	120	147	138
45-50	60	-	50	-	55	63	-	81	-	72	70	-	40	61	57
50-55	36	-	-	-	36	29	-	26	-	28	12	-	-	-	12
10-80	16685	16783	14798	15915	16045 16025	11144	11736	12056	12217	11788 11781	7788	7984	7809	7676	7814 7813

$l_i - l_{i+1}$	29					30					31			
(mm)	A33/A90		A10/A67		Mean	A9/A66		A32/A89		Mean	A82	A3/A104		Mean
10-12	904	997	949	889	935	1982	2288	1733	1595	1900	2690	3105	3848	3214
12-14	736	789	763	769	764	1899	1939	1791	1859	1872	4657	4387	5367	4804
14-16	628	658	649	656	648	1741	1902	1581	1506	1683	4073	4078	4217	4123
16-18	567	592	593	664	604	1547	1424	1574	1370	1479	3460	3660	4124	3748
18-20	490	450	527	506	493	1281	1312	1224	1215	1258	2852	3513	3549	3305
20-25	891	880	900	916	897	2508	2583	2453	2260	2451	5739	6133	6275	6050
25-30	580	620	557	654	603	1732	1742	1639	1512	1656	3425	4213	3926	3855
30-35	380	-	384	393	386	981	977	-	912	957	1854	2090	-	1972
35-40	266	-	254	-	260	527	485	-	364	459	642	} 976	-	642
40-45	131	-	124	-	128	-	188	-	170	179	206		-	206
45-50	57	-	53	-	55	-	61	-	73	67	49	97	-	73
50-55	-	-	15	-	15	-	21	-	-	21	26	-	-	26
10-80	5661	5849	5767	5898	5794 5793	14470	14924	13536	12858	13947 13924	29482	32249	34466	32066 32000

$l_i - l_{i+1}$	32					33					34				
(mm)	A42/A83		A60/A26		Mean	B14/B84		B35/B61		Mean	B12/B55		B46/B75		Mean
10-12	2823	2554	2141	2740	2565	593	781	719	745	710	505	568	500	488	515
12-14	3153	3141	2907	3265	3117	821	1056	904	1051	958	575	527	413	479	499
14-16	2511	2725	2680	2737	2663	939	1043	1070	1029	1020	404	490	430	436	440
16-18	2166	2314	2400	2503	2346	1048	1386	1035	1196	1166	456	414	402	397	417
18-20	1950	2035	2105	2005	2024	1299	1514	1254	1377	1361	351	436	389	375	388
20-25	3685	3765	3675	4177	3826	3188	2958	3696	3815	3414	966	1035	945	955	975
25-30	2405	2460	2518	2693	2519	2493	3800	2823	2520	2909	826	837	815	809	822
30-35	760	1020	1202	-	994	2036	-	1989	1741	1922	593	-	747	538	626
35-40	550	-	444	-	497	828	-	833	910	857	212	-	-	225	219
40-45	180	-	149	-	165	-	-	228	-	228	74	-	-	111	93
45-50	50	-	72	-	61	-	-	110	-	110	-	-	-	45	45
50-55	-	-	31	-	31	-	-	40	-	40	-	-	-	-	-
10-80	20170	20571	20327	22021	20772 20759	13534	15614	14710	14833	14673 14670	5045	5269	5052	4886	5063 5061

$l_i - l_{i+1}$ (mm)	35					36					37				
	B18/B66		B33/B82		Mean	B16/B63		B31/B83		Mean	A16/A94		A40/A71		Mean
10-12	352	331	351	302	334	1135	1306	1079	1090	1153	2848	2458	2990	2115	2603
12-14	257	236	229	253	244	1105	1261	1079	1094	1135	4394	5024	4463	3230	4278
14-16	218	210	226	219	218	1359	1177	1016	1037	1147	3874	4434	4675	3502	4121
16-18	207	212	187	205	203	1103	1188	1072	1140	1126	3148	3787	3756	2850	3385
18-20	160	166	174	162	166	943	1142	773	945	951	2542	2960	2710	2682	2724
20-25	349	326	380	360	354	1855	1596	1473	1674	1650	4373	4695	-	4109	4392
25-30	312	303	235	263	278	890	1126	915	830	940	2558	2615	-	2257	2477
30-35	215	197	196	201	202	461	-	750	-	606	1200	-	-	1505	1353
35-40	-	137	120	122	126	-	-	232	-	232	633	-	-	612	623
40-45	-	49	51	-	50	-	-	97	-	97	189	-	-	149	169
45-50	-	21	22	-	22	-	-	53	-	53	-	-	-	-	-
50-55	-	11	9	-	10	-	-	-	-	-	-	-	-	-	-
10-80	2289	2170	2186	2179	2206 2205	9271	9667	8161	8660	8940 8921	25856	28092	27418	23203	26142 26072

$l_i - l_{i+1}$ (mm)	38					39					40				
	A13/A70		A29/A86		Mean	A14/A64		A53/A87		Mean	A17/A95		A41/A72		Mean
10-12	1370	1364	1558	1492	1446	790	851	940	799	845	2627	2869	3292	3684	3118
12-14	1438	1496	1468	1370	1443	766	737	813	694	753	2961	2858	3102	2751	2918
14-16	1920	1654	1332	1237	1536	619	613	560	664	614	2667	2742	3128	2843	2845
16-18	698	883	1112	1253	987	560	525	497	527	527	1958	2226	2115	2524	2206
18-20	1033	1057	957	1066	1028	476	468	436	445	456	1897	1916	2037	1843	1923
20-25	2070	2043	2015	2063	2048	802	856	879	890	857	3557	3640	3752	3744	3673
25-30	1496	1434	1266	1400	1399	474	597	611	547	557	2025	2224	2344	2158	2188
30-35	888	835	781	878	846	416	412	406	337	393	984	-	1110	1033	1042
35-40	-	455	355	-	405	253	219	-	234	235	408	-	439	443	430
40-45	-	158	176	-	167	93	-	-	107	100	159	-	-	161	160
45-50	-	46	56	-	51	57	-	-	42	50	40	-	-	55	48
50-55	-	-	21	-	21	25	-	-	17	21	-	-	-	24	24
10-80	11572	11423	11101	11371	11367 11365	5384	5445	5546	5307	5421 5420	19290	20071	21356	21278	20499 20480

$l_i - l_{i+1}$ (mm)	41	42					43					44				
	A59	B17/B79		B32/B64		Mean	A18/A96		A36/A73		Mean	B9/B58		B26/B86		Mean
10-12	1509	522	577	460	591	538	1594	1630	1431	1507	1541	797	594	786	771	737
12-14	2237	463	492	409	488	463	1214	1626	1330	1321	1373	720	682	703	670	694
14-16	2376	463	430	393	415	425	1292	1453	1341	1363	1362	655	630	548	651	621
16-18	2145	406	439	380	433	415	924	1285	1204	1009	1106	663	560	557	566	587
18-20	1826	379	368	367	327	360	942	1164	946	994	1012	637	599	535	546	579
20-25	3565	842	944	701	846	833	1986	2173	1894	1950	2001	1349	1382	1184	1304	1305
25-30	2362	743	847	680	782	763	1349	-	1472	1336	1386	1074	1015	1014	1082	1046
30-35	1316	643	643	555	-	614	821	-	867	882	857	923	956	856	962	924
35-40	655	372	-	261	-	316	368	-	382	422	391	713	706	649	682	688
40-45	237	102	-	93	-	98	159	-	150	-	155	-	-	175	-	175
45-50	136	27	-	28	-	28	64	-	58	-	61	-	-	91	-	91
50-55	36	-	-	28	-	28	21	-	-	-	21	-	-	-	-	-
10-80	18413	4975	5254	4359	4861	4862 4851	10737	12116	10941	11002	11199 11184	7921	7514	7127	7529	7523 7518

$l_i - l_{i+1}$ (mm)	45					46					47				
	A45/A101		A30/A93		Mean	B37/B56		B11/B74		Mean	A19/A74		A37/A97		Mean
10-12	2451	2576	2881	3083	2748	2394	2550	2384	2135	2366	6337	8573	5516	5980	6602
12-14	2092	2354	2392	2498	2334	1980	2320	2027	2125	2113	6089	4672	5924	5668	5588
14-16	2128	2219	2251	2242	2210	2225	2150	2180	2210	2191	4780	4741	4701	4317	4635
16-18	1861	1914	1930	2093	1950	1827	2162	1765	1726	1870	4179	4353	4138	3869	4135
18-20	1740	1745	1802	1812	1775	1508	1508	1802	1296	1529	3700	3839	3498	3110	3537
20-25	3610	3670	3721	3830	3708	-	2340	-	1860	2100	6771	6948	6284	6050	6513
25-30	2664	2689	2640	2778	2693	-	1465	-	945	1205	2963	3523	3801	3025	3328
30-35	1716	1899	1810	1829	1814	-	493	-	619	556	1542	-	-	1369	1456
35-40	1010	-	994	-	1002	-	337	-	339	338	596	-	-	447	522
40-45	456	-	490	-	473	-	139	-	204	172	203	-	-	233	218
45-50	115	-	139	-	127	-	81	-	87	84	81	-	-	71	76
50-55	-	-	54	-	54	-	23	-	24	24	-	-	-	-	-
10-80	19870	20674	21121	21859	20881 20869	14916	15572	14239	13573	14575 14556	37266	39096	35995	34152	36627 36583

Table 8 Crack propagation records of the additional flight-simulation tests. Values of Δn in numbers of flights.

First column: crack length interval
First and second line: Test series No. and Specimen No.
Mean values are arithmetical averages.

Material 7075-T6 Clad

$l_i - l_{i+1}$ (mm)	13a			15a			17a				
	B44/B62		Mean	B36/B49		Mean	B87/B95		B6/B13		Mean
5- 6	381	495	438	434	404	419	260	317	333	318	307
6- 7	590	509	550	432	408	420	250	285	274	236	261
7- 8	439	402	421	334	286	310	222	186	231	226	216
8- 9	425	430	428	264	270	267	162	183	194	191	183
9-10	386	353	370	263	317	290	185	182	185	214	192
10-12	761	737	749	417	409	413	224	240	266	224	239
12-14	819	744	782	398	480	439	204	202	232	211	212
14-16	1021	903	962	394	367	381	189	185	199	218	197
16-18	1009	1237	1123	331	375	353	137	140	161	145	146

Material 2024-T3 Alclad

$l_i - l_{i+1}$ (mm)	25a			27a			29a		
	A46/A102		Mean	A23/A76		Mean	A7/A57		Mean
6- 7	2354	1663	2008	1446	1531	1489	932	1072	1002
7- 8	2888	2926	2907	1168	938	1053	712	781	746
8- 9	2697	2658	2677	1059	993	1026	649	706	677
9-10	2637	2878	2757	954	885	920	568	586	577
10-12	5175	5047	5111	1817	1681	1749	948	1016	982
12-14	3947	4358	4152	1448	1493	1470	738	829	783

Table 9 Crack propagation records of the constant-amplitude tests. Values of Δn in cycles.
First column: Crack length interval. Second line: stress amplitude in kg/mm^2.
Third line: specimen No. Mean values are arithmetical averages.

	7075-T6								2024-T3									
$l_i - l_{i+1}$ (mm)	S_a=2.2			S_a=1.1					S_a= 8.8	S_a= 6.6	S_a= 4.4	S_a=2.2			S_a=1.1			
	B19/B7		Mean	B6/B13		B80/B93		Mean	A61	A55	A54	A50/A105		Gem.	A44	A7/A57		Mean
10-12	4941	5277	5109	-	-	56410	34168	45289	855	1795	4220	23700	21785	22743	247080	-	-	247080
12-14	3361	3320	3341	-	-	21545	26035	23790	558	1470	3195	15700	18470	17085	155240	-	-	155240
14-16	2942	2708	2825	-	-	17200	19735	18468	338	1145	2790	14320	13590	13955	101735	-	-	101735
16-18	2396	2465	2431	-	-	12005	14495	13250	210	945	1930	11315	11880	11598	89740	73219	91344	84768
18-20	2230	2250	2240	-	-	12035	12405	12220	185	620	1790	8920	10185	9553	70615	67695	59066	65792
20-25	4315	4475	4395	23600	19900	20205	23790	21874	240	1200	3040	17455	17215	17335	124945	112803	121636	119795
25-30	3165	3248	3207	16795	16000	14985	15443	15806	140	715	1855	12363	11765	12064	86805	76322	77489	80205
30-35	2645	2726	2686	11850	11250	11330	10838	11317	73	-	1140	8152	-	8152	52340	52143	51020	51834
35-40	2213	2121	2167	9085	8480	8555	7960	8520	22	-	645	5320	-	5320	39815	36475	-	38145
40-45	1506	1805	1656	-	6160	6330	9555	6148	-	100	310	3333	-	3333	27255	24760	-	26008
45-50	924	-	924	-	4370	4855	4105	4443	-	-	-	2127	-	2127	19190	17565	-	18378
50-55	-	-	-	-	3170	3200	2955	3108	-	-	-	1100	-	1100	10430	11185	-	10808
10-80	31274	31955	31615	-	-	191951	180948	186450	2653	8626	21165	124306	125423	124865	1031470	-	-	1031470

Table 10 Crack propagation records for the 2024-T3 specimens with a central hole

l (mm)	48								49			
	A 27	/	A 62		A 56	/	A110		A 20	/	A 75	
12	21055	23542	19906	14560	19291	18604	19400	25858	18304	12285	19603	15698
14	23542	24980	21143	16869	20845	20279	22206	28078	19195	13903	20239	16914
16	26237	27347	23387	20000	22731	22280	25081	30073	20032	15432	21065	18522
18	28882	30078	25745	22543	-	24693	28052	32426	21025	-	22078	19868
20	31572	32219	27347	24835	27185	26722	30428	34271	22188	18904	22943	21025
25	-	-	31000	29805	31365	31086	34983	-	23856	21611	24863	23599
30	-	-	33666	32616	34247	33881	-	-	25188	23838	26057	25220
35	-	-	34950	34380	35571	35407	-	-	25882	25078	-	26311
40	-	-	35455	35276	36130	36087	-	-	26204	25851	-	-
45	-	-	35534	35427	36328	36283	-	-	26307	26220	-	-
50	-	-	35594	35566	36385	36371	-	-	26339	26300	-	-
55	-	-	35615	35608	36394	36388	-	-		26335	-	-
80	41422	41422	35617	35617	36396	36396	41792	41792		26354	27480	27480

l (mm)	49				50							
	A 38	/	A 98		A 21	/	A 77		A 15	/	A 92	
12	14328	17458	13576	15842	15491	13976	12360	14980	14278	12700	11202	12654
14	15295	18548	15105	16644	16096	14614	13047	15421	14910	13520	11888	13160
16	16644	19488	16374	17627	16560	15311	13856	15834	15402	14252	12674	13653
18	18216	20326	17404	18600	16988	15918	14448	16194	15828	14880	13180	14044
20	19382	21223	18548	19495	17382	16447	-	-	16243	15402	13738	14436
25	21793	23033	20802	21352	-	17492	16270	17145	-	-	14783	15153
30	-	-	22308	22740	-	-	17014	17492	-	-	15453	15657
35	-	-	23365	23574	-	-	17477	17736	-	-	15840	15954
40	-	-	23843	-	-	-	17718	17866	-	-	16057	16136
45	-	-	23960	24033	-	-	17858	17943	-	-	16186	16227
50	-	-	24043	24051	-	-	17936	17970	-	-	16243	16230
55	-	-	-	-	-	-	17965					
80	25392	25392	24056	24056	19112	19112	17981	17981	18004	18004	16268	16260

Values in the tables are numbers of flights as counted from the beginning of the test. For each specimen two values are given, corresponding to the cracks at both sides of the hole. The first column gives the crack length as measured from the center of the hole. First and second line: Test series No. and specimen No.

Table 11 Effect of taxiing loads

Values of stresses in kg/mm^2

Material	$S_{a,max}$	$S_{a,min}$	Crack propagation life (flights) (a) – Taxiing loads applied: yes (b)	no (b)	Life ratio (yes/no)
7075	8.8	1.1	13406 (1)	13329 (4)	0.99
	7.7		8719 (4)	9565 (4)	1.10
	6.6		5889 (5)	5062 (6)	0.86
	6.6	3.3	9863 (4)	9779 (4)	0.99
2024	7.7	1.1	15921 (1)	16025 (4)	1.01
	6.6		10876 (5)	11781 (4)	1.08
	7.7	3.3	31000 (1)	32000 (3)	1.03
	6.6		20513 (4)	20759 (4)	1.01
				Average	1.01

(a) Mean values drawn from table 7. The numbers between brackets indicate the number of tests carried out.

(b) In both cases S_{min} in the GTAC is equal to $-3.4\ kg/mm^2$.
For the taxiing loads $S_m \pm S_a = -2 \pm 1.4\ kg/mm^2$.

Table 12 Effect of the minimum stress in the GTAC

Values of stresses in kg/mm^2

Material	$S_{a,max}$	$S_{a,min}$	Crack propagation life (flights) (a), S_{min} in the GTAC: -1.4 (TL)	-3.4 (TL)	-3.4 (No TL)	Life ratio (-1.4/-3.4)
7075	7.7	1.1	9617 (1)	8719 (4)	9565 (4)	1.1
	6.6	1.1	4800 (1)	5889 (5)	5062 (6)	0.9
	5.5	1.1	3075 (1)	-	3538 (4)	0.9
	4.4	1.1	2714 (1)	-	2385 (4)	1.1
2024	6.6	1.1	16308 (1)	10876 (5)	11781 (4)	1.4
	4.4	1.1	6516 (2)	-	5793 (4)	1.1

(a) See table 11.

Table 13 Effect of omitting small gust loads

Values of stresses in kg/mm^2

Material	TL	Gusts: Sequence	$S_{a,max}$	Crack propagation life (flights) (a), $S_{a,min}$ of the gust cycles: 1.1	2.2	3.3	Life ratios (b): 1.1	2.2	3.3
7075	yes	Random	6.6	5889 (5)		9863 (4)	1		1.67
	no		7.7	9565 (4)		21179 (2)	1		2.21
	no		6.6	5062 (6)	7006 (4)	9779 (4)	1	1.38	1.93
	no	Programmed	6.6	5061 (4)		8921 (4)	1		1.76
2024	yes	Random	7.7	15921 (1)		31000 (1)	1		1.95
	no		6.6	10876 (5)		20513 (4)	1		1.89
	no		7.7	16025 (4)		32000 (3)	1		2.00
	no		6.6	11781 (4)	13924 (4)	20759 (4)	1	1.18	1.76
	no	Programmed	6.6	11365 (4)		20480 (4)	1		1.80

(a) See table 11.

(b) The life for $S_{a,min} = 1.1\ kg/mm^2$ was taken as being 1.

Table 14 Effect of truncating the gust spectrum

Values of stresses in kg/mm^2

Test conditions					Crack propagation life (flights) [a]					Life ratios [b]				
					$S_{a,max}$ of gust cycles					$S_{a,max}$ of gust cycles				
Material	Load sequence	Taxiing loads	GTAC S_{min}	Gusts $S_{a,min}$	8.8	7.7	6.6	5.5	4.4	8.8	7.7	6.6	5.5	4.4
7075	Random	yes	-1.4	1.1		9617 (1)	4600 (1)	3075 (1)	2714 (1)		2.00	1	0.64	0.57
			-3.4		13406 (1)	8719 (4)	5889 (5)			2.28	1.48	1		
		no	-3.4	1.1	13329 (4)	9565 (4)	5062 (6)	3538 (4)	2385 (4)	2.63	1.89	1	0.70	0.47
				3.3		21179 (2)	9779 (4)				2.17	1		
	Program	no	-3.4	1.1	14670 (4)		5061 (4)		2205 (4)	2.90		1		0.44
2024	Random	yes	-1.4	1.1			16308 (1)		6516 (2)			1		0.40
			-3.4			15921 (1)	10876 (5)				1.46	1		
			-3.4	3.3		31000 (1)	20513 (4)				1.51	1		
		no	-3.4	1.1	23292 (4)	16025 (4)	11781 (4)	7813 (4)	5793 (4)	1.98	1.36	1	0.66	0.49
				3.3		32000 (3)	20759 (4)				1.54	1		
	Program	no	-3.4	1.1	26072 (4)		11365 (4)		5420 (4)	2.29		1		0.48

(a) Mean values drawn from table 7. The numbers between brackets indicate the numbers of tests carried out.

(b) The life for $S_{a,max}$ = 6.6 kg/mm^2 was taken as being 1.

Table 15 Comparison between the random and the programmed flight simulation tests.

Values of stresses in kg/mm^2. GTAC without GL.

Test conditions			Crack propagation life (a) (flights)		Life ratio
Material	Gust cycles		Random gust sequence	Programmed gust sequence	Programmed/Random
	$S_{a,min}$	$S_{a,max}$			
7075	1.1	8.8	13329 (4)	14670 (4)	1.10
		6.6	5062 (6)	5061 (4)	1.00
		4.4	2385 (4)	2205 (4)	0.92
	3.3	6.6	9779 (4)	8921 (4)	0.91
2024		8.8	23292 (4)	26072 (4)	1.12
		6.6	11781 (4)	11365 (4)	0.96
		4.4	5793 (4)	5420 (4)	0.94
	3.3	6.6	20759 (4)	20480 (4)	0.99
				Average	0.99

(a) See table 16.

Table 16 Effects of reversing the gust cycles of applying one gust per flight and of omitting the GTAC.

Gust cycles in random sequence ($S_{a,max}$ = 6.6 kg/mm^2). GTAC without TL

Characteristic test conditions (see also fig.3)	$S_{a,min}$ of gusts (kg/mm^2)	Crack propagation life(a) (flights)		Relative crack propagation life(b)	
		7075	2024	7075	2024
Standard random sequence	1.1	5062 (6)	11781 (4)	1	1
Reversed gust cycles	1.1	4851 (4)	11184 (4)	0.96	0.95
Small gusts omitted	2.2	7006 (4)	13924 (4)	1.38	1.18
	3.3	9779 (4)	20759 (4)	1.93	1.76
Only one gust per flight(c)	-	14556 (4)	36583 (4)	2.88	3.10
GTAC omitted	1.1	7518 (4)	20869 (4)	1.49	1.77

(a) Mean values drawn from table 7. The numbers between brackets indicate the number of tests carried out.
(b) The life for the standard random sequence was taken as being 1.
(c) The largest positive gust load of each flight was applied.

Table 17 Comparison between the two alloys

Values of stresses in kg/mm^2

Test conditions				Crack propagation life (flights) (a)		Life ratio
Gust sequence	Taxiing loads	Gust cycles				
		$S_{a,min}$	$S_{a,max}$	7075	2024	(2024)/(7075)
Random	yes	1.1	7.7	8719 (4)	15921 (1)	1.8
			6.6	5889 (5)	10876 (5)	1.8
		3.3	6.6	9863 (4)	20513 (4)	2.1
	no	1.1	8.8	13329 (4)	23292 (4)	1.7
			7.7	9565 (4)	16025 (4)	1.7
			6.6	5062 (6)	11781 (4)	2.3
			5.5	3538 (4)	7813 (4)	2.2
			4.4	2385 (4)	5793 (4)	2.4
		2.2	6.6	7006 (4)	13924 (4)	2.0
		3.3	7.7	21179 (2)	32000 (3)	1.5
			6.6	9779 (4)	20759 (4)	2.1
		(b)	6.6	14556 (4)	36583 (4)	2.5
		1.1(c)	6.6(c)	4851 (4)	11184 (4)	2.3
Random, no GTAC	-	1.1	6.6	7518 (4)	20869 (4)	2.8
Programmed		1.1	8.8	14670 (4)	26072 (4)	1.8
			6.6	5061 (4)	11365 (4)	2.2
			4.4	2205 (4)	5420 (4)	2.5
		3.3	6.6	8921 (4)	20480 (4)	2.3
					Average	2.1

(a) Mean values drawn from table 7. The numbers between brackets indicate the numbers of tests carried out.

(b) Only one gust load (the largest one) per flight.

(c) Gust cycles in reversed sequence.

Table 18 **Damage calculations for test series No.45**

Material: 2024-T3 Alclad

$S_{a,max} = 6.6\ kg/mm^2$

$S_{a,min} = 1.1\ kg/mm^2$

GTAC omitted

S_a (kg/mm^2)	1.1	2.2	3.3	4.4	5.5	6.6	7.7(a)	8.8(a)
n/N in 5000 flights(b)	0.145	0.312	0.115	0.077	0.016	0.006	0.003	0.002

(a) Not applied in test series No.45.
(b) n from table 5, N from fig.15.

Sum of damage increments for S_a = 1.1 - 6.6 is 0.808.

Predicted life : $\frac{1}{0.808} \cdot 5000 = 6188$ flights

Crack propagation life in tests = 20869 flights

} Test result corresponds to $\sum \frac{n}{N} = 3.4$

Table 19 **Fatigue life reduction if small gust cycles are included.**
Comparison between tests and predictions.

M = crack propagation life **with** small gust cycles included.
M'= crack propagation life **without** small gust cycles.
The predicted M values have been calculated from M' and the constant-amplitude test data, see section

Material	Test conditions			Small gust cycles S_a-values	M/M' (percentage)		Ratio
	Taxiing loads	$S_{a,max}$	Load sequence		test	predicted	test/predicted
7075	yes	6.6	Random	1.1 and 2.2	60	20	3.0
	no	7.7			44	10	4.4
		6.6			52	20	2.6
		6.6	Programmed		47	22	2.1
		6.6	Random	1.1	72	47	1.5
2024	yes	7.7	Random	1.1 and 2.2	51	26	2.0
		6.6			53	35	1.5
	no	7.7			50	25	2.0
		6.6			57	35	1.6
		6.6	Programmed		55	35	1.6
		6.6	Random	1.1	85	71	1.2

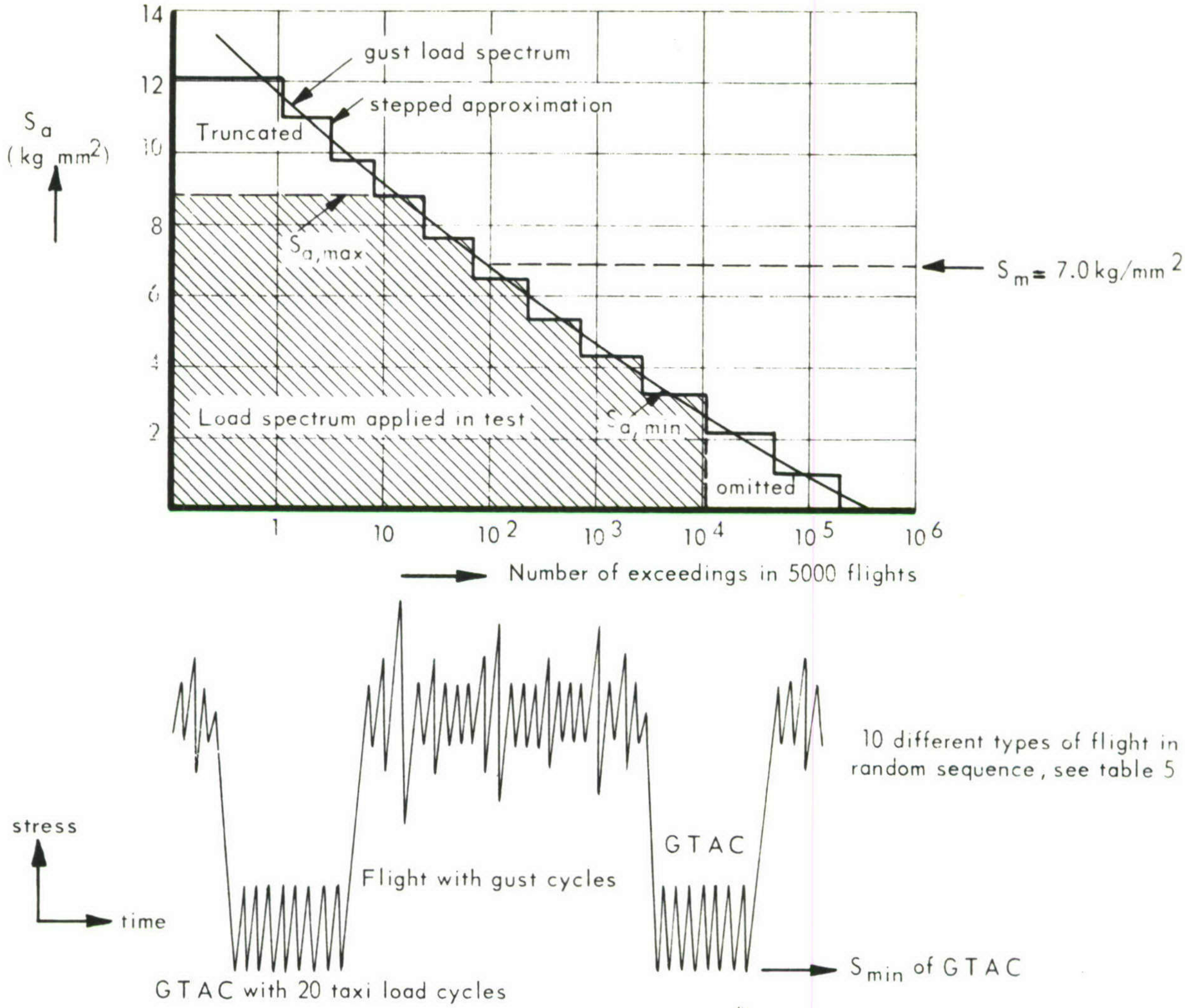

Note : Each gust cycle consisted of a positive gust followed by a negative gust of equal amplitude (exept for tests with reversed gust cycles)

	Variables of test program (see also fig. 3)
Gust load spectrum	$S_{a,\,max}$ (truncation) $S_{a,\,min}$ (omission of many small cycles)
GTAC	S_{min} (2 values)
Taxiing loads	Omission of taxiing loads (same S_{min})
Flight profile	Omission of GTAC Only one gust cycle per flight
Sequence	Random Gust cycles in reversed sequence Programmed per flight
Material	2 Aℓ – alloys , 2024 – T 3 and 7075 – T 6

FIG. 1 SURVEY OF VARIABLES STUDIED IN THE PRESENT TEST SERIES.

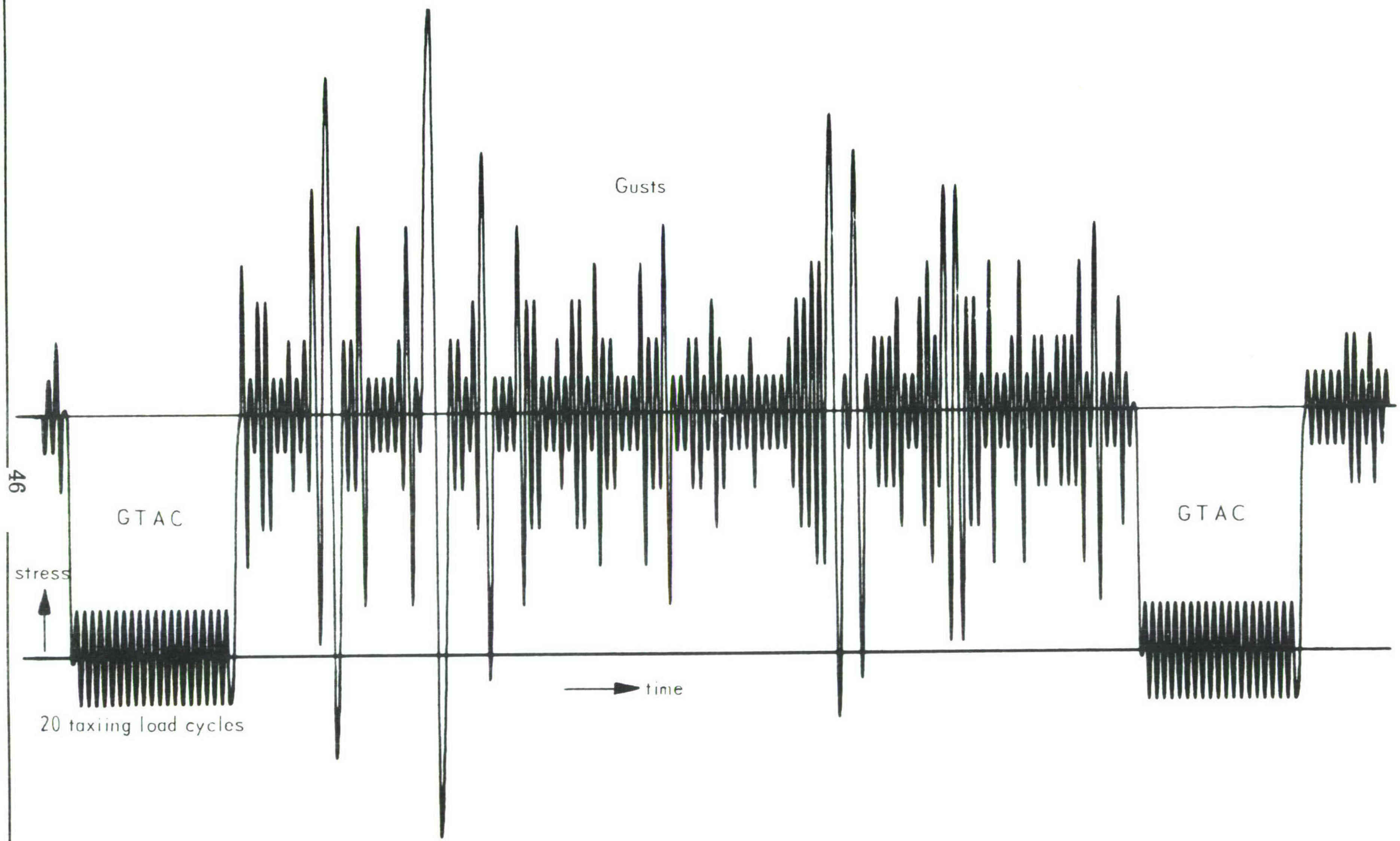

FIG. 2 THE LOAD SEQUENCE IN THE MOST SEVERE FLIGHT (TYPE A)

FIG. 3 LOAD RECORDS OF FLIGHT No. 19 (TYPE F) FOR DIFFERENT TYPES OF FLIGHT SIMULATION

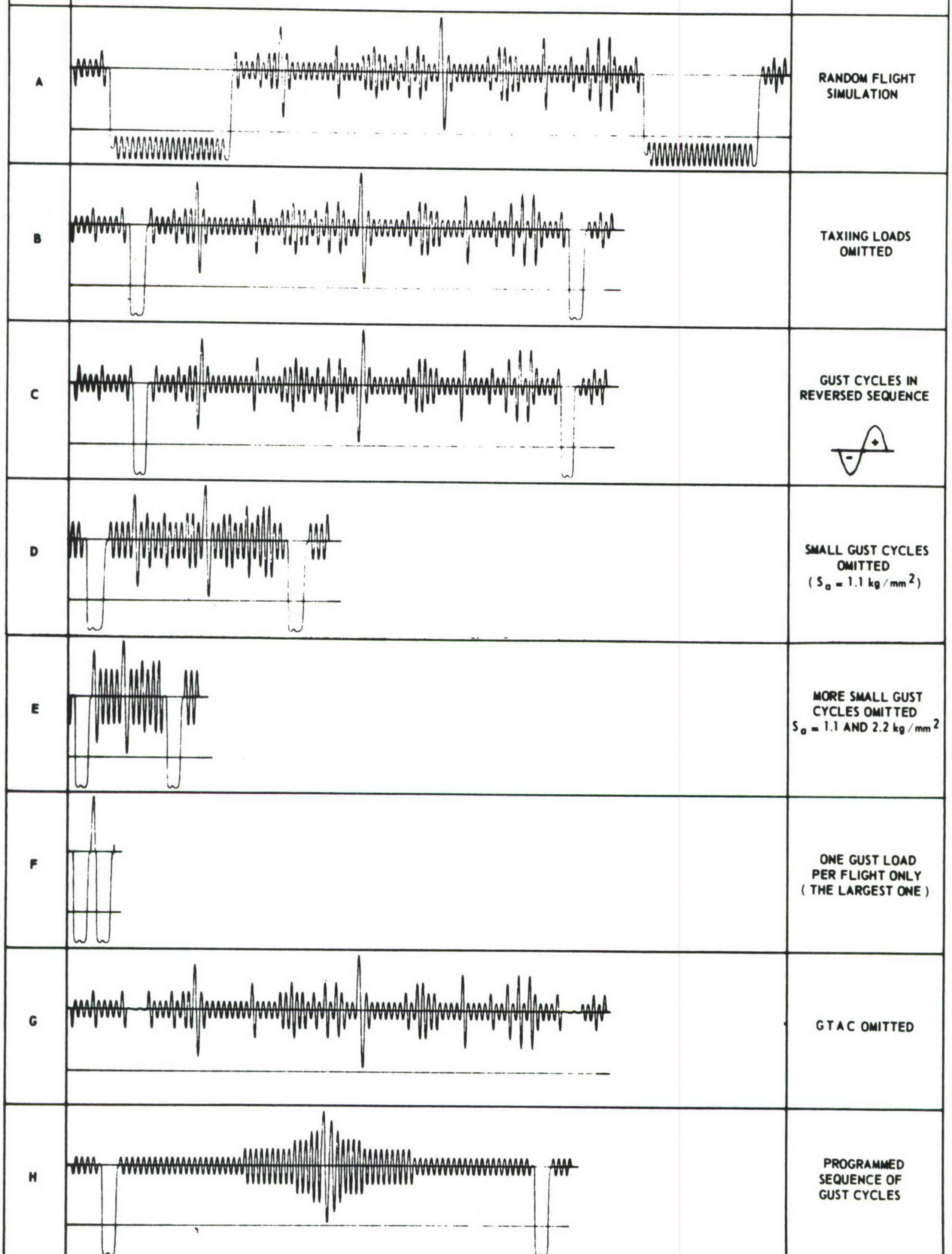

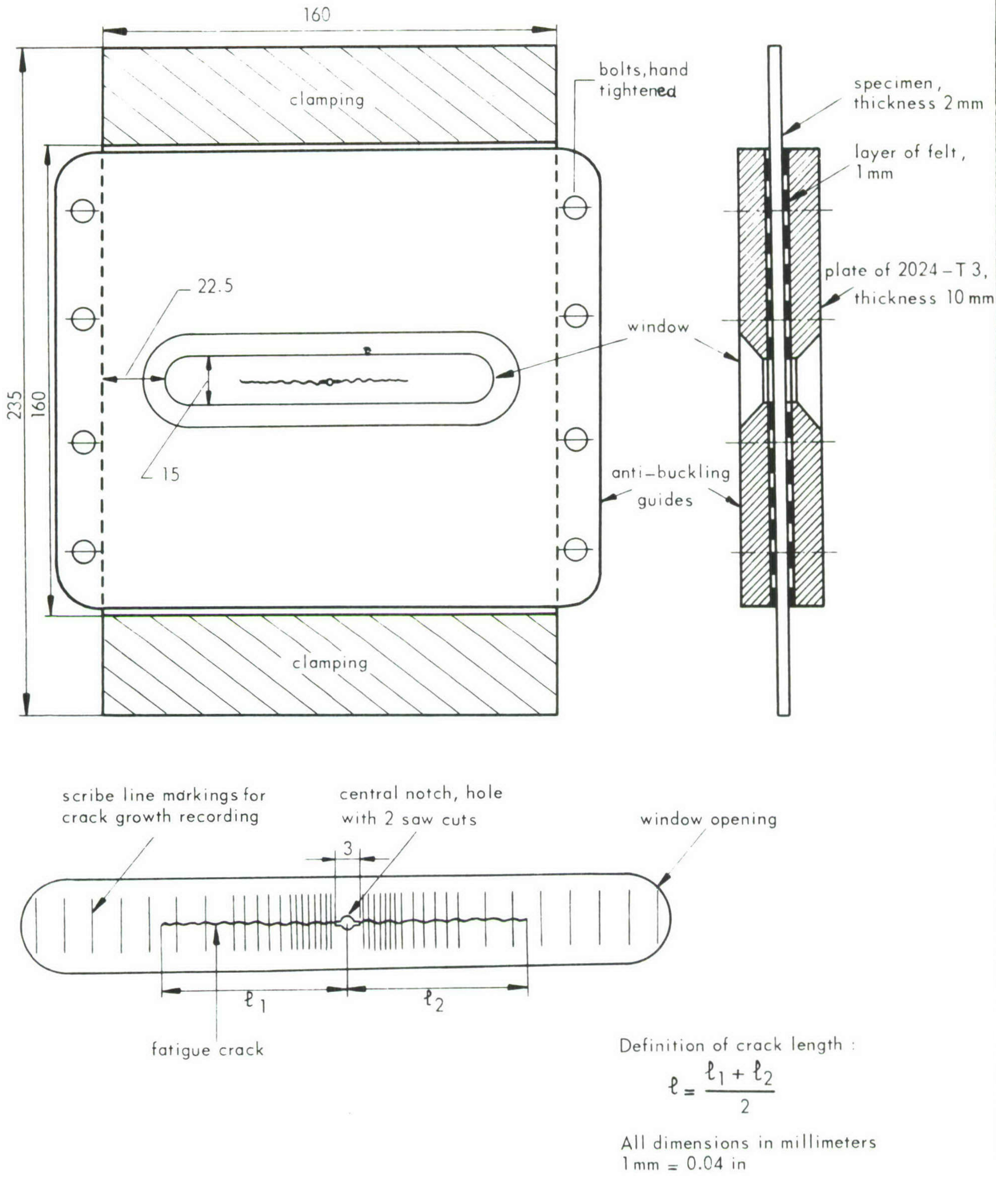

FIG. 4 DIMENSIONS OF THE SPECIMEN AND ANTI – BUCKLING GUIDES

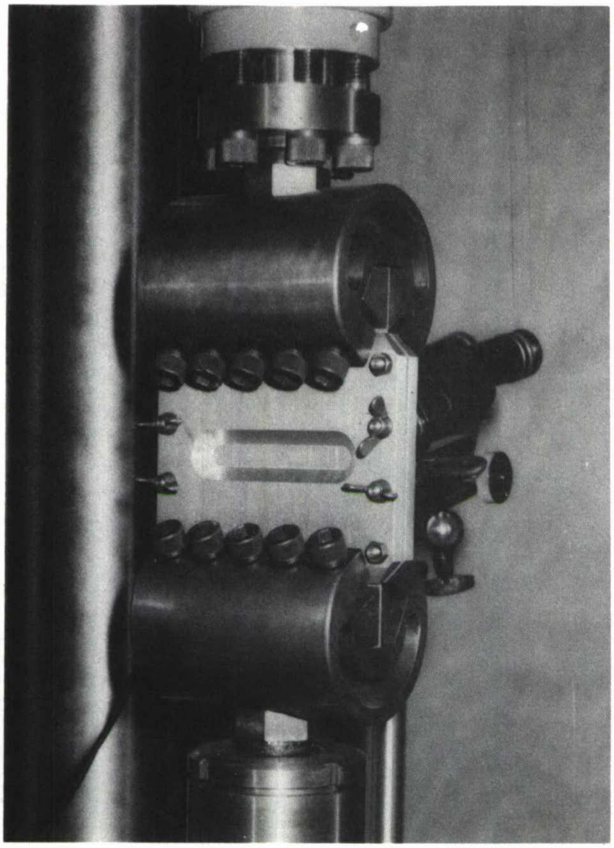

FIG. 5

PICTURE OF THE SPECIMEN, ANTI-BUCKLING GUIDES WITH WINDOW AND CLAMPINGS. STEREO-MICROSCOPE (30 x) FOR CRACK OBSERVATION IN THE BACKGROUND.

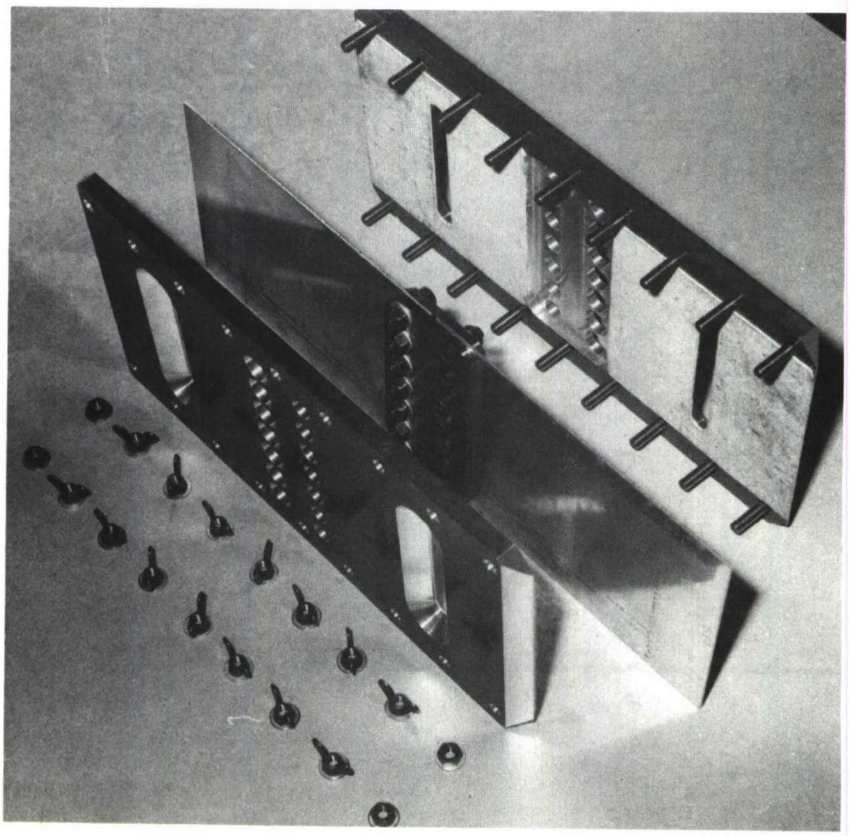

FIG. 6 TWO SPECIMENS CONNECTED BY A DOUBLE STRAP JOINT, ANTI-BUCKLING GUIDES COVERED BY FELT AT THE INNER SIDE AND PROVIDED WITH TWO WINDOWS EACH.

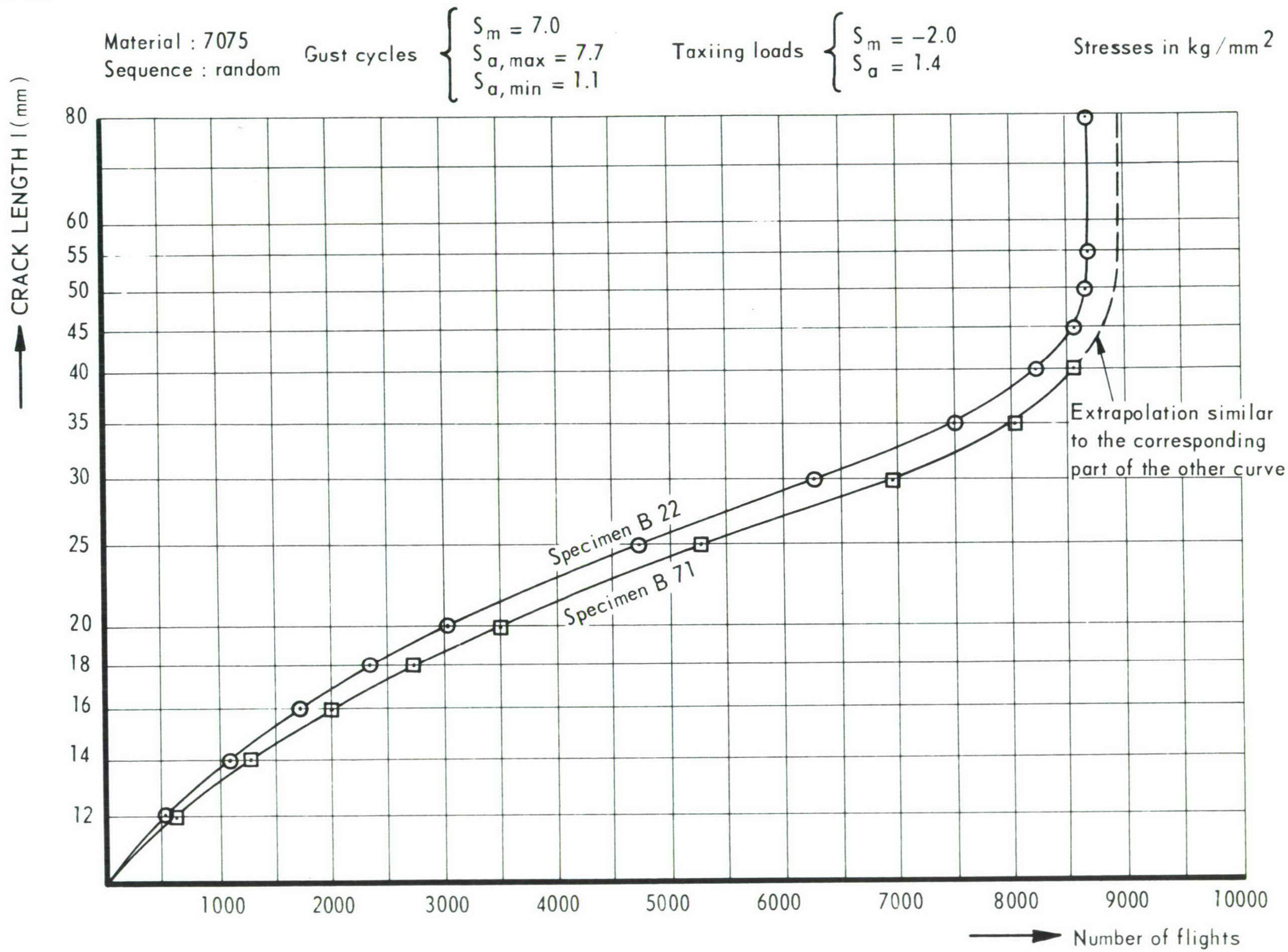

FIG. 7 EXAMPLE OF TWO CRACK PROPAGATION CURVES FOR TWO SPECIMENS SIMULTANEOUSLY TESTED IN SERIES

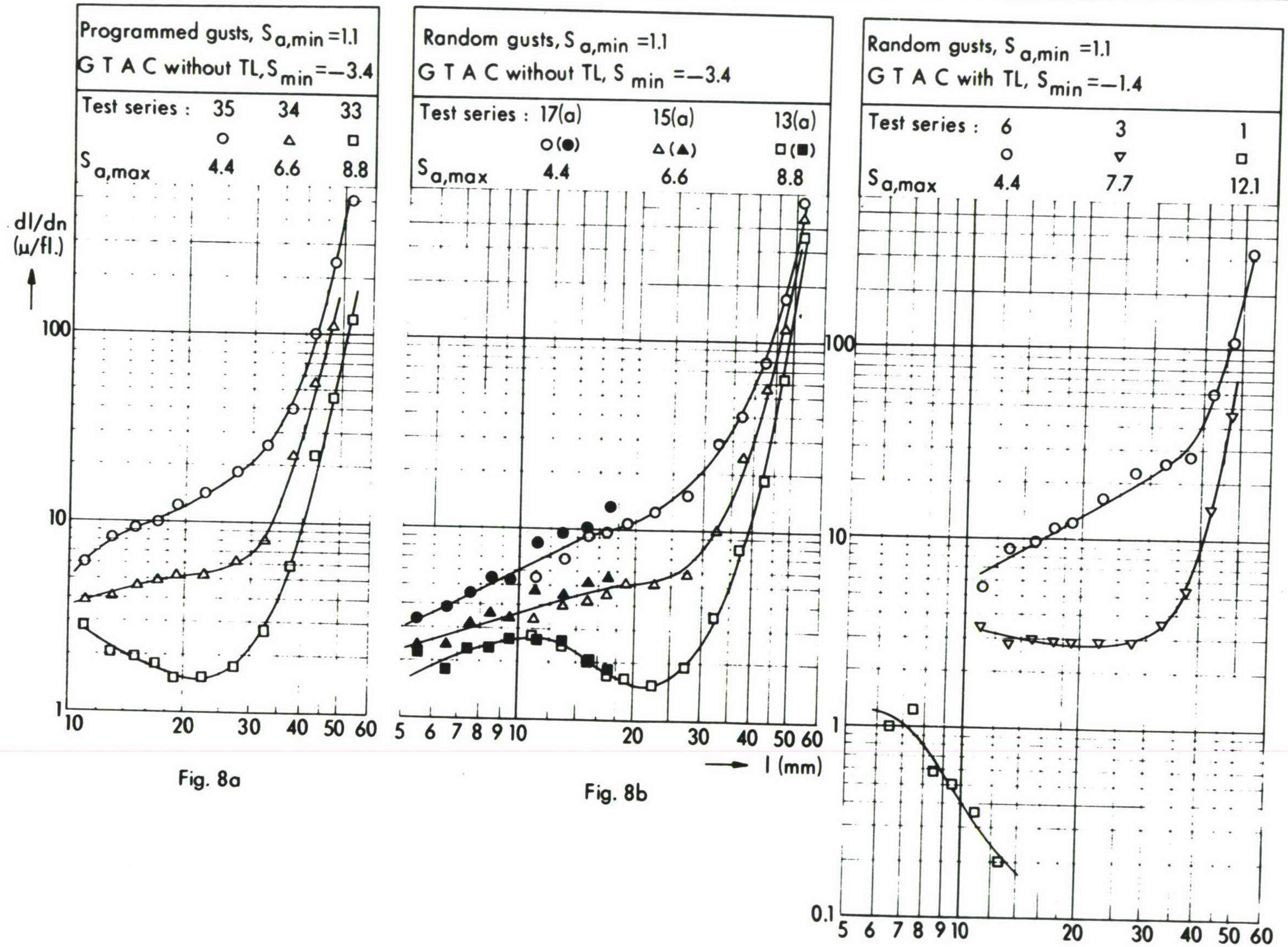

Fig. 8a

Fig. 8b

Fig. 8c

FIG. 8 EFFECT OF TRUNCATION ($S_{a,max}$) ON THE CRACK PROPAGATION RATE

MATERIAL 7075–T6

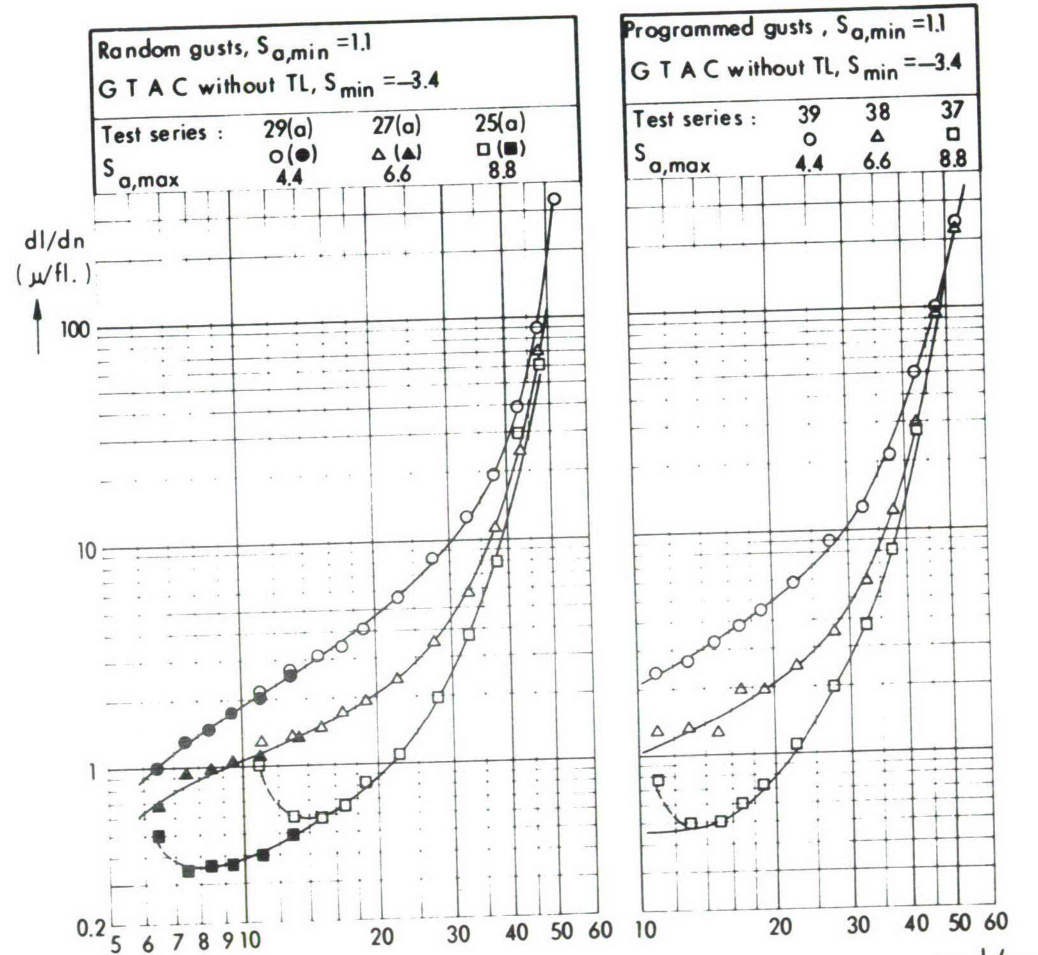

Fig. 8d

Fig. 8e

FIG. 8 , CONTINUED. MATERIAL 2024—T3

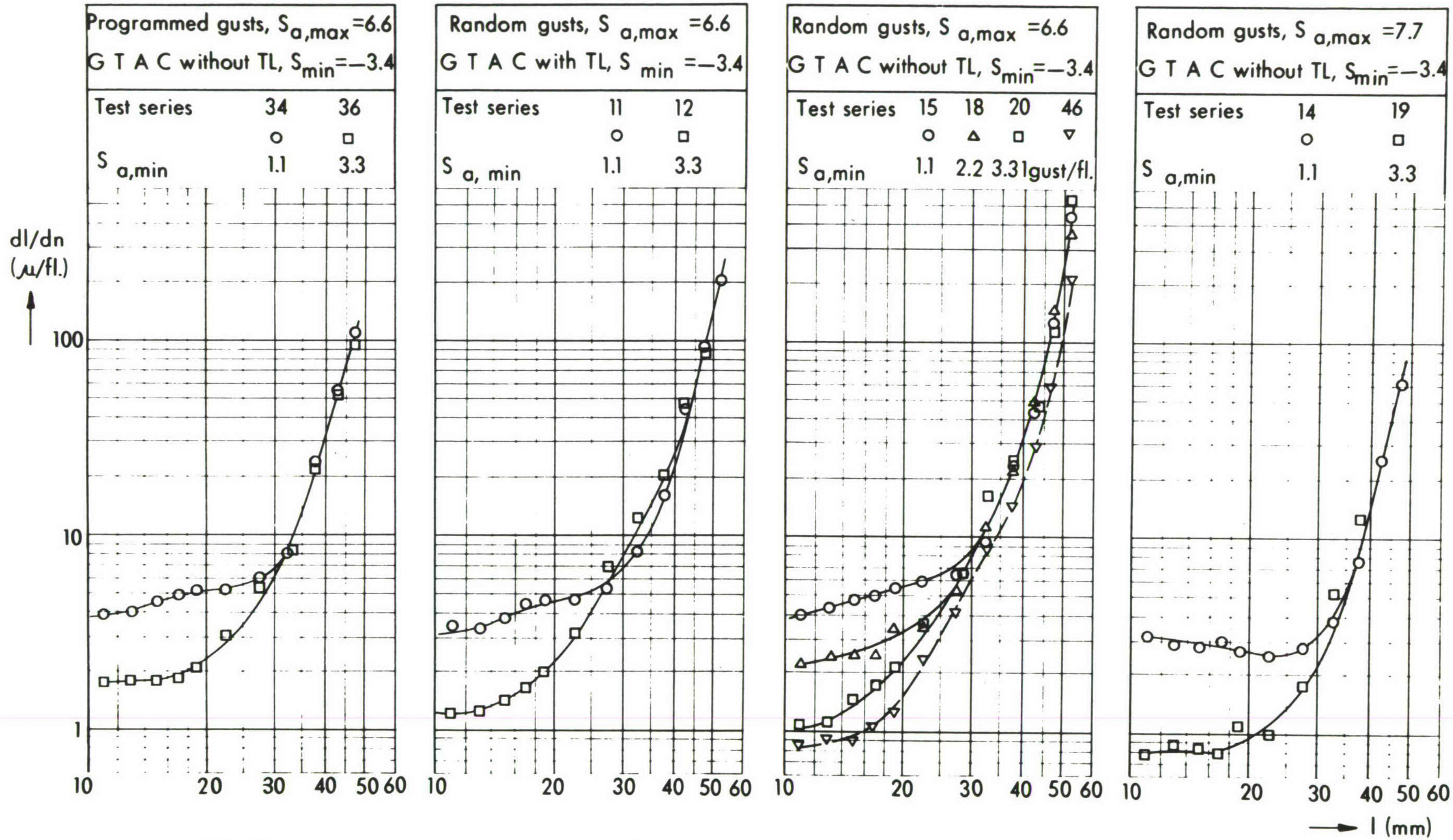

Fig. 9a

Fig. 9b

Fig. 9c

Fig. 9d

FIG. 9 EFFECT OF OMITTING SMALL GUST LOADS ON THE CRACK PROPAGATION RATE

MATERIAL 7075–T6

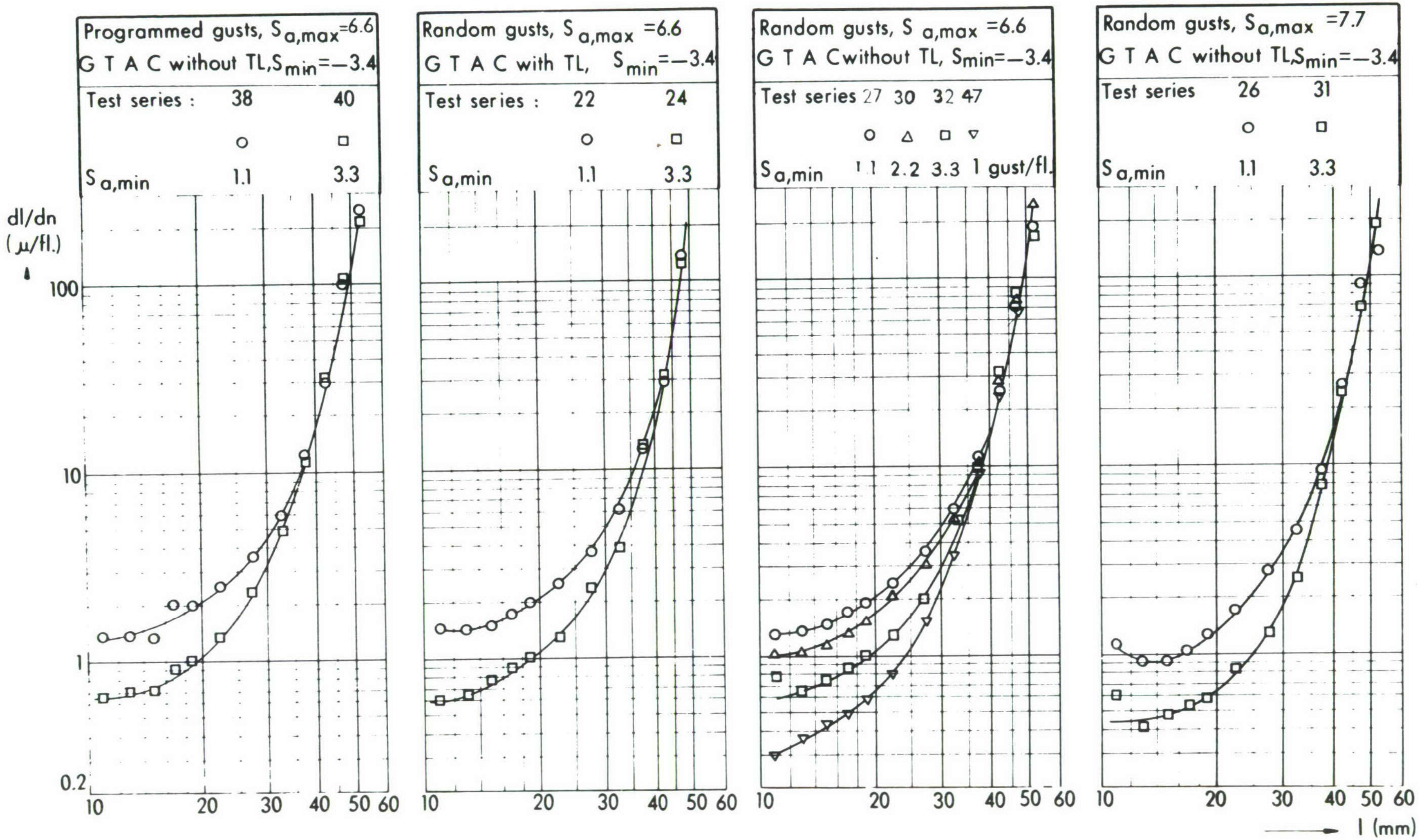

Fig. 9e Fig. 9f Fig. 9g Fig. 9h

FIG. 9 , CONTINUED MATERIAL 2024—T3

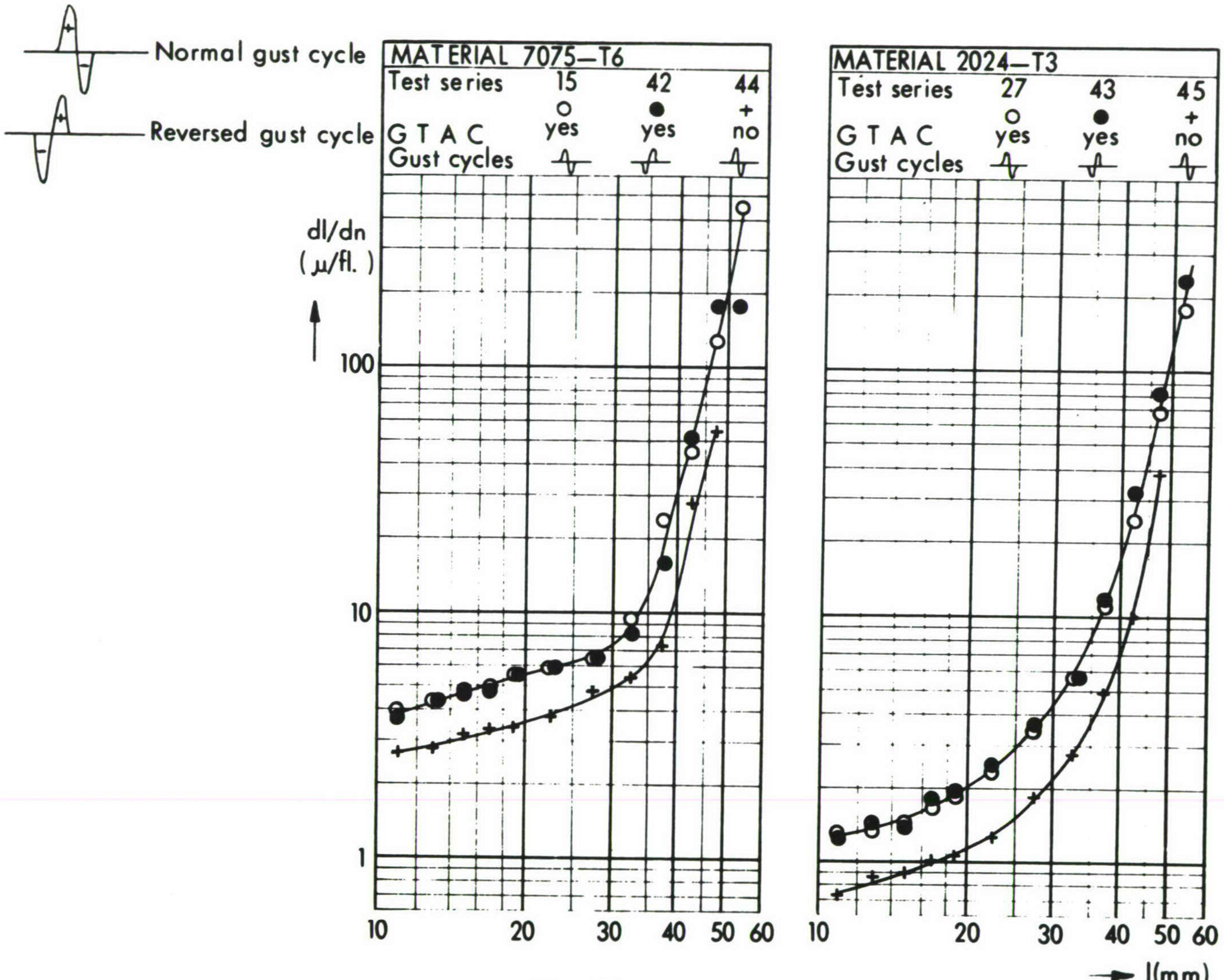

Fig. 10a

Fig. 10b

FIG. 10 THE EFFECTS OF OMITTING THE G T A C
AND OF REVERSING THE GUST CYCLES ON THE CRACK PROPAGATION RATE

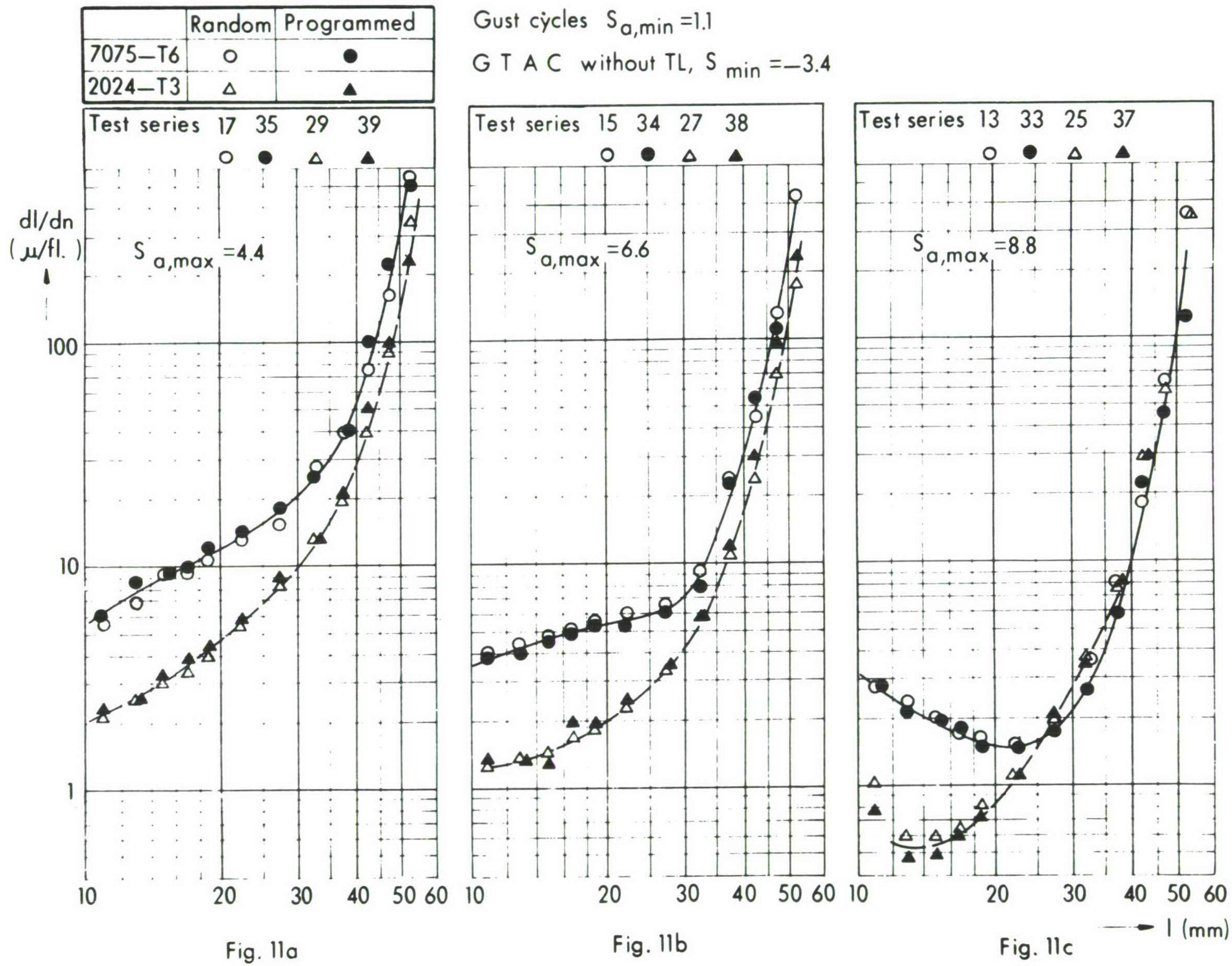

FIG. 11 COMPARISON BETWEEN THE CRACK RATES FOR RANDOM AND PROGRAMMED FLIGHT SIMULATION

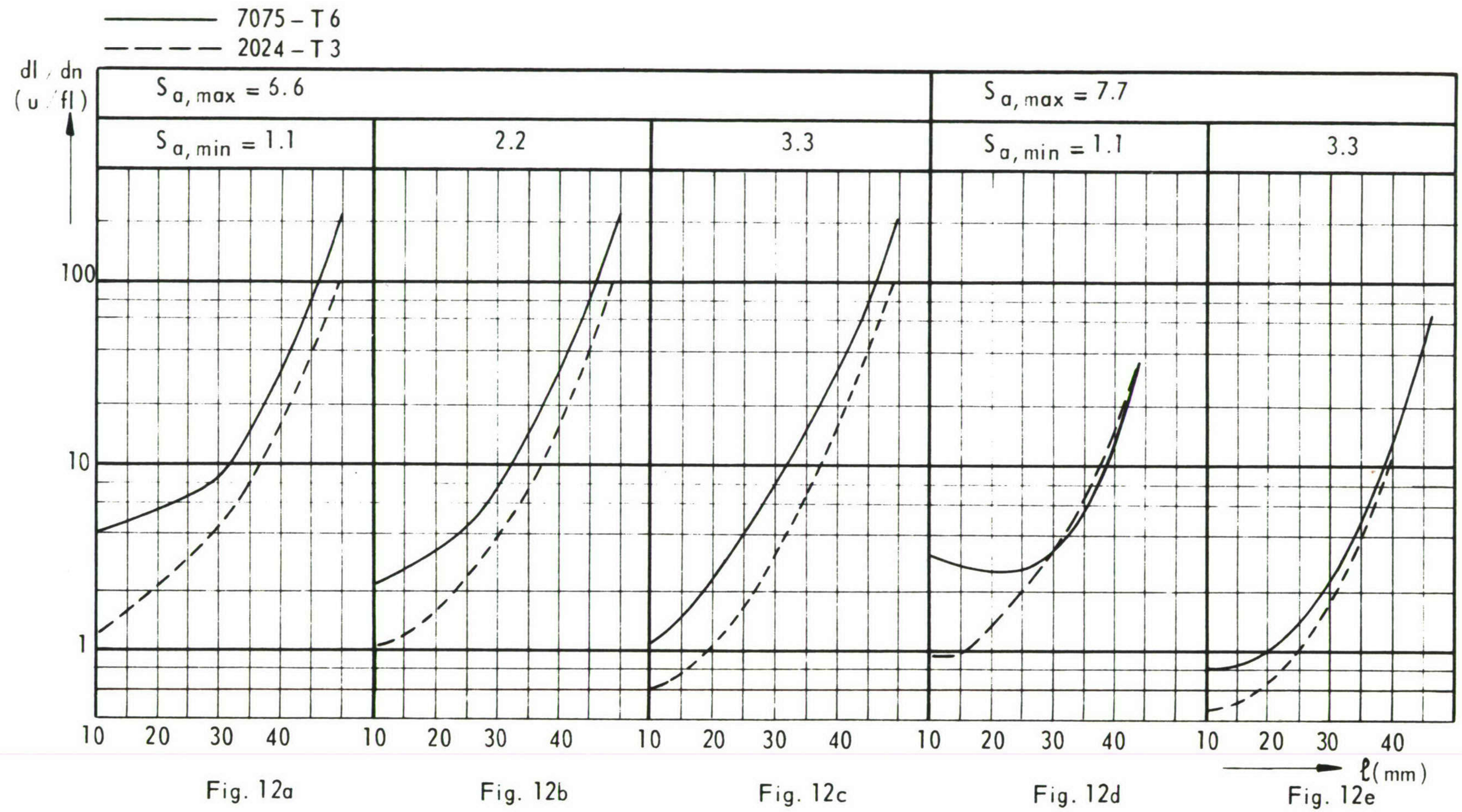

FIG. 12 COMPARISON BETWEEN THE CRACK RATES IN THE TWO ALLOYS. EFFECT OF $S_{a,max}$ AND $S_{a,min}$, SEE ALSO FIG. 11. RANDOM GUSTS, GTAC WITHOUT TL , $S_{min} = -3.4$

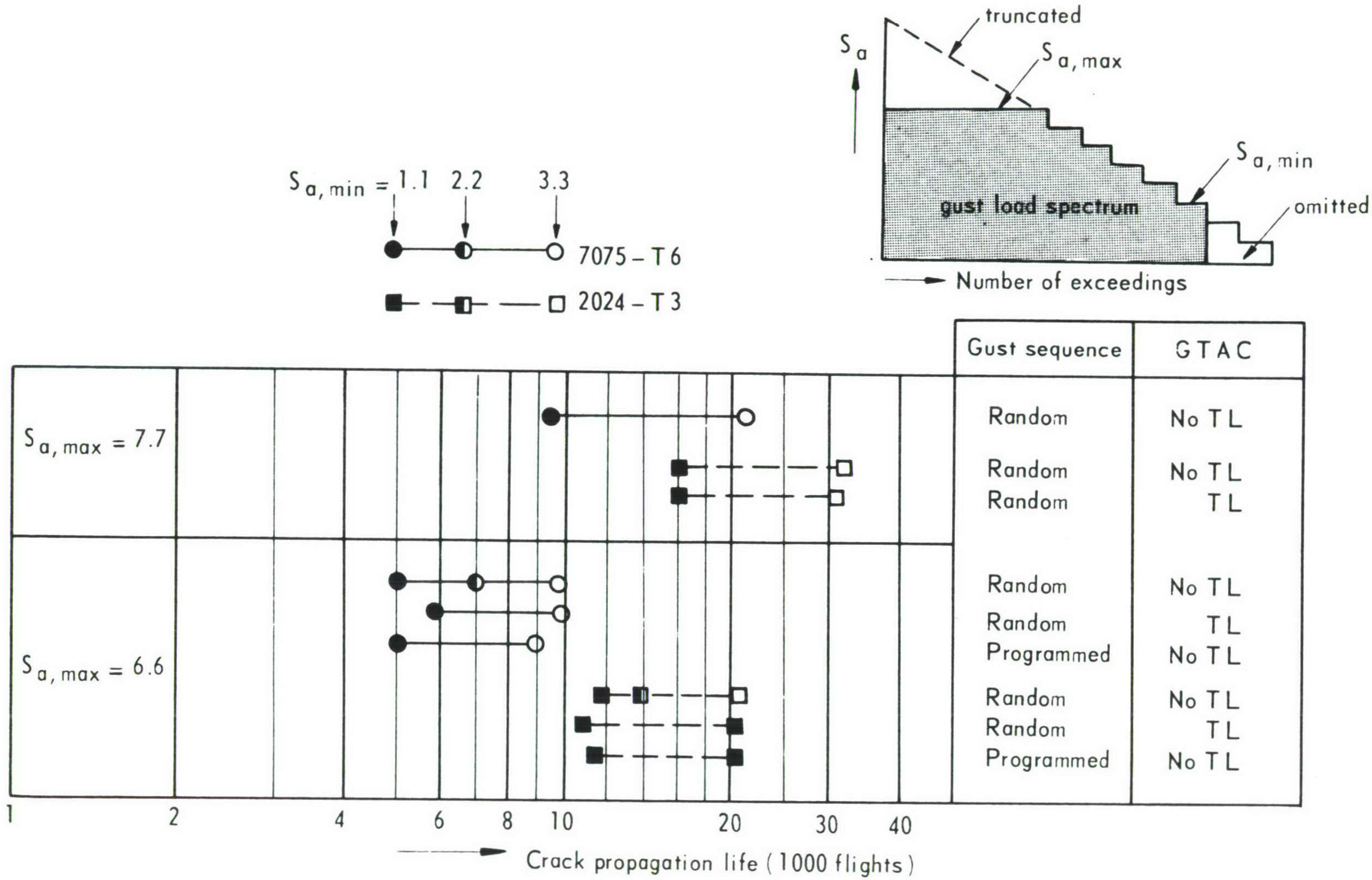

FIG. 13 THE EFFECT OF OMITTING SMALL GUST LOADS ON THE CRACK PROPAGATION LIFE.

7075–T6	2024–T3	GTAC S_{min}	TL	SEQUENCE
○	●	−3.4	no	random
□	■	−3.4	no	programmed
△	▲	−3.4	yes	random
▽	▼	−1.1	yes	random

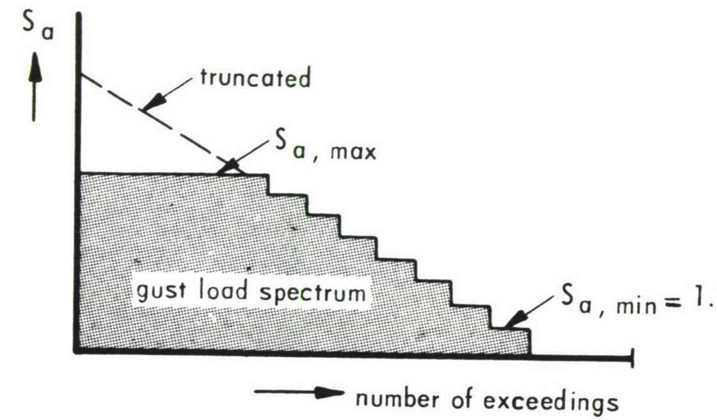

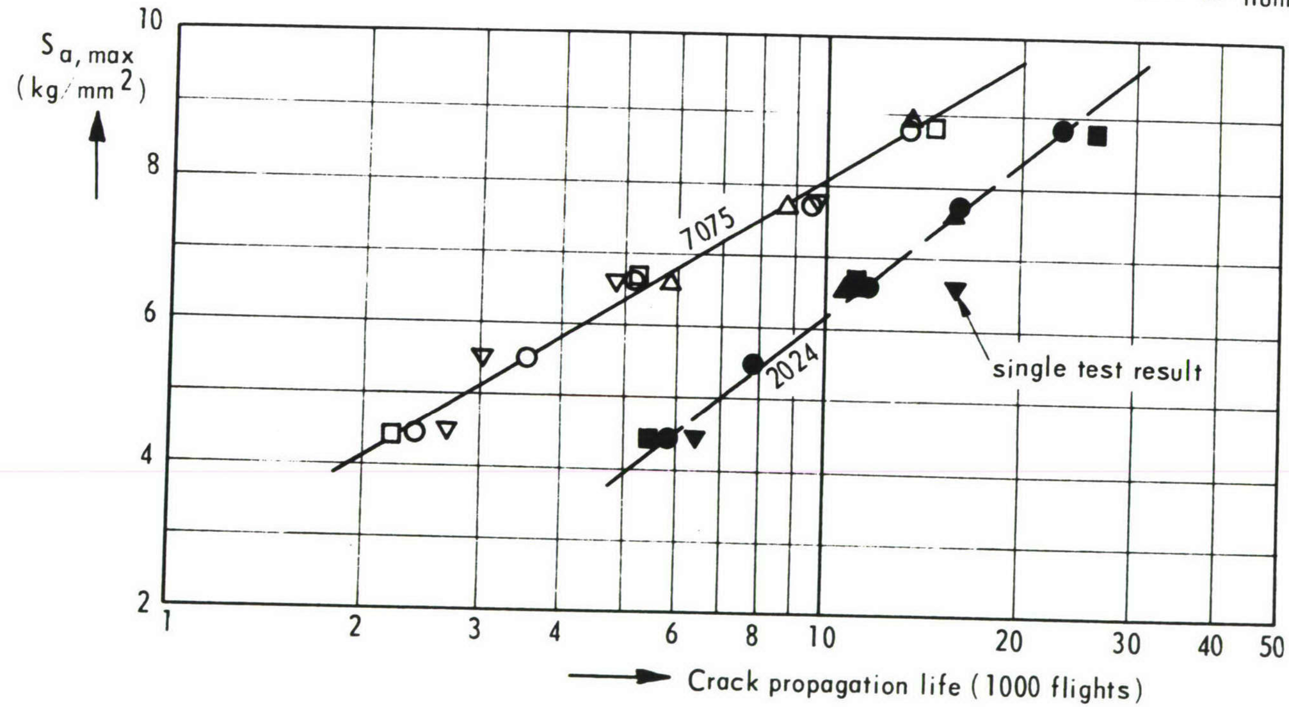

FIG. 14 THE EFFECT OF TRUNCATING THE GUST LOAD SPECTRUM ON THE CRACK PROPAGATION LIFE

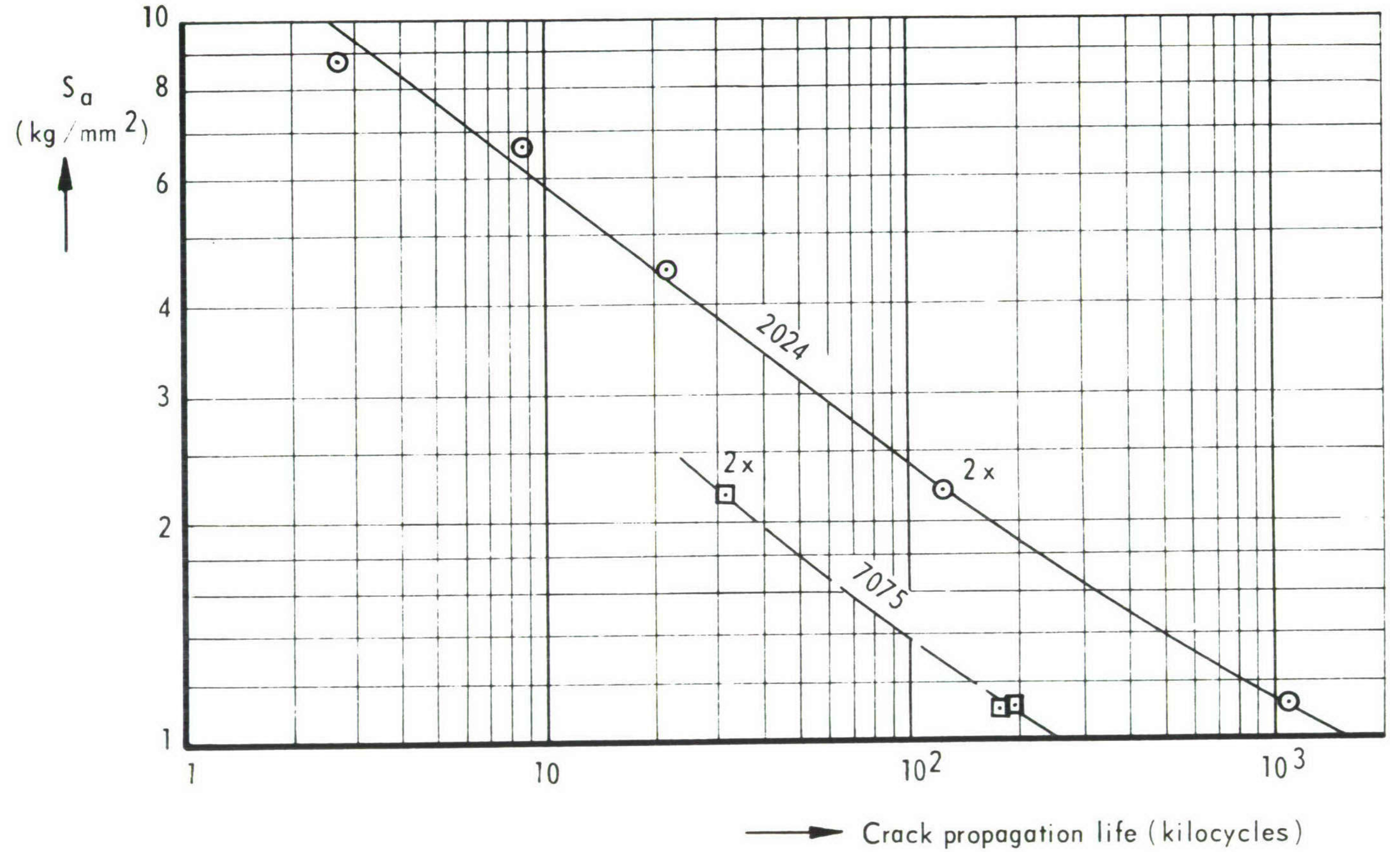

FIG. 15 THE CONSTANT-AMPLITUDE TEST DATA PLOTTED AS S-N CURVES

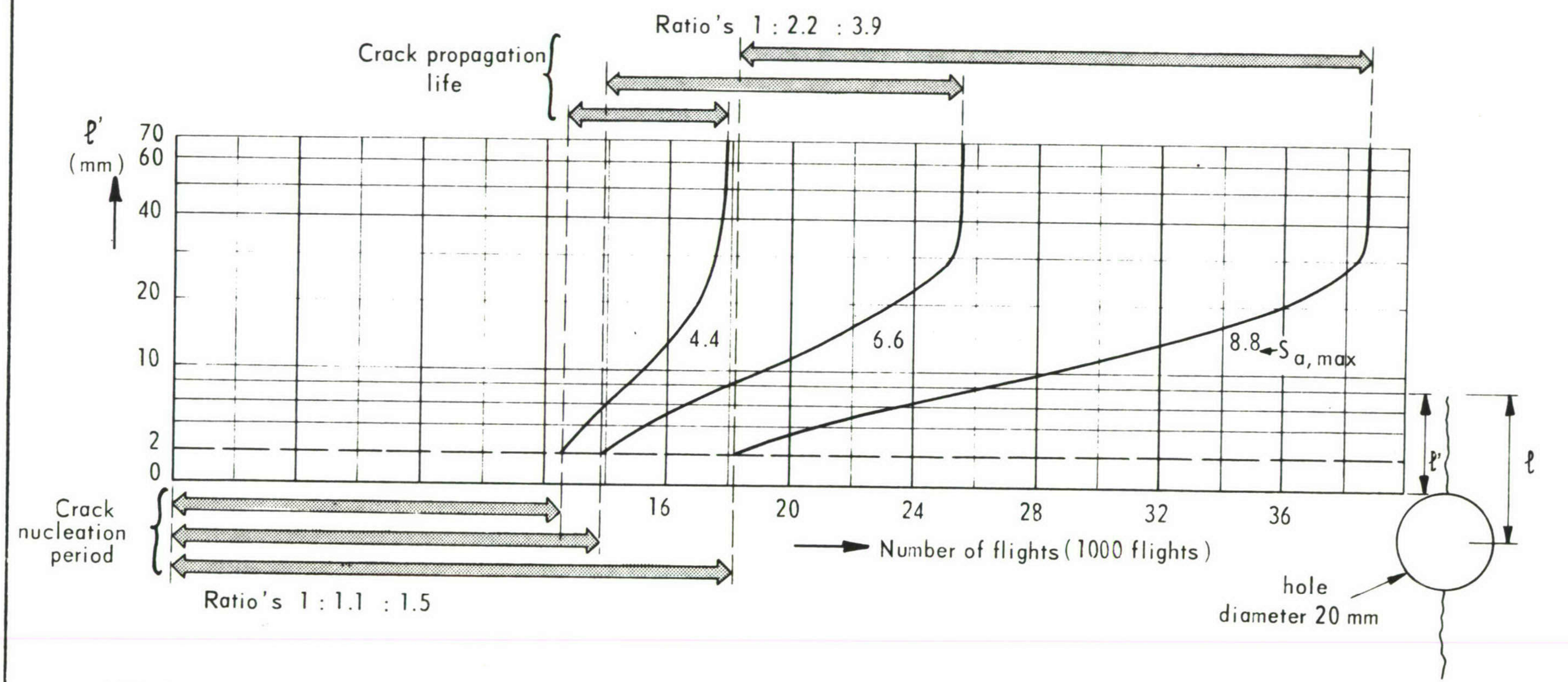

FIG. 16 CRACK PROPAGATION CURVES FOR THE 2024–T3 SPECIMENS WITH A CENTRAL HOLE. EFFECT OF TRUNCATION LEVEL ($S_{a,max}$) ON THE CRACK-NUCLEATION PERIOD (TO $\ell' = 2$ mm) AND THE CRACK PROPAGATION LIFE.

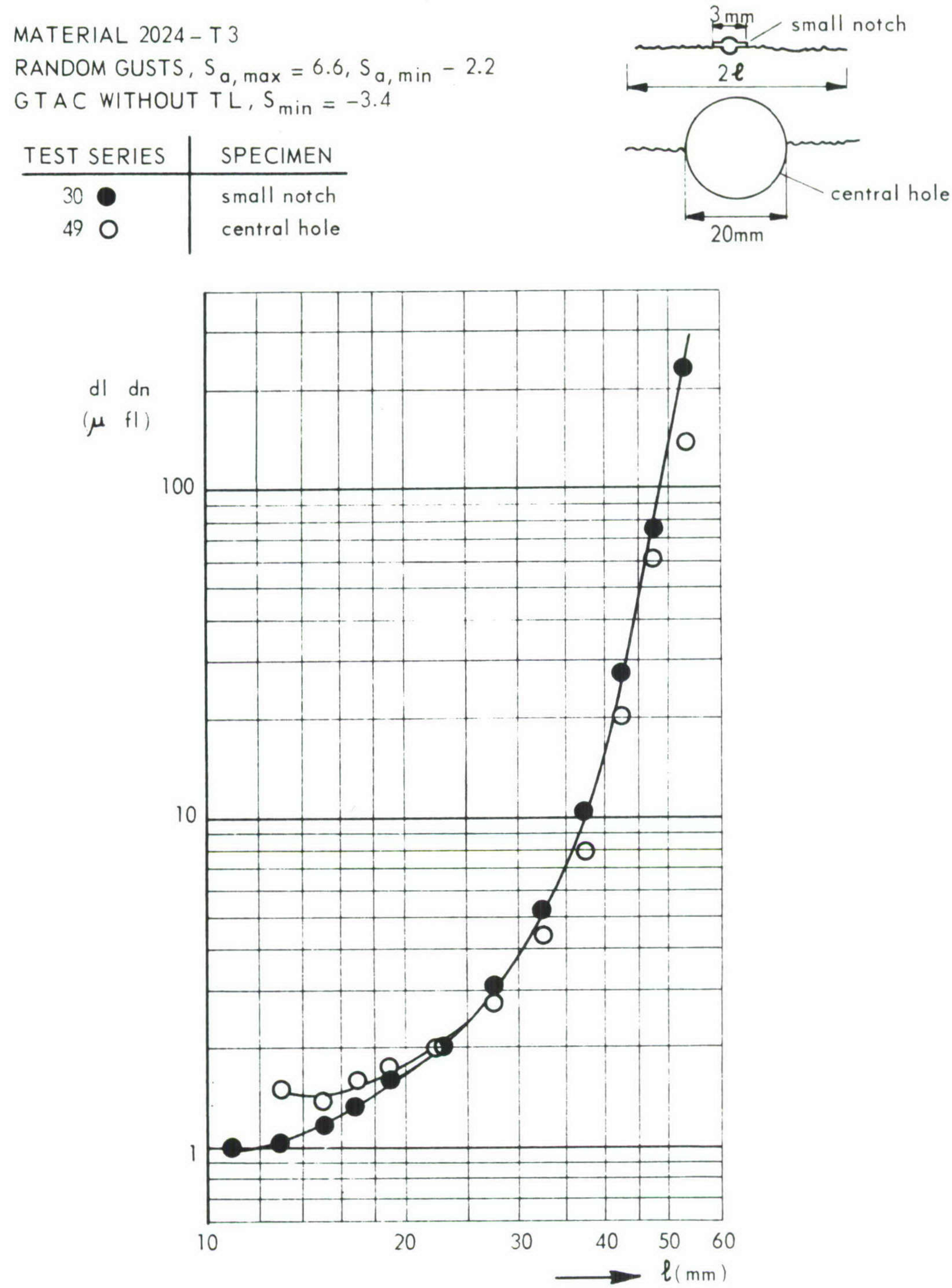

FIG. 17 COMPARISON BETWEEN THE CRACK PROPAGATION RATES IN SPECIMENS WITH A SMALL NOTCH OR A CENTRAL HOLE

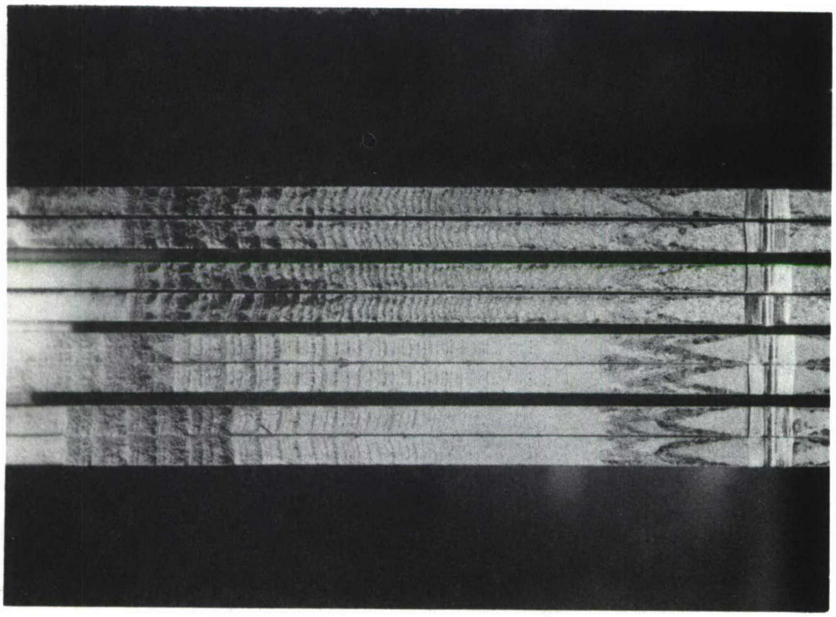

Random
Programmed
7075-T6
Random
Programmed
2024-T3

$S_{a,max} = 8.8\ kg/mm^2$

$S_{a,min} = 1.1\ kg/mm^2$

GTAC without TL,
$S_{min} = -3.4\ kg/mm^2$

Magnification 2 x

Central notch at right side of picture

Fig.18 Fracture surfaces of 4 specimens showing macro fatigue bands.

Specimen B47, 7075-T6
Random flight simulation.
$S_{a,max}$ = 6.6 kg/mm^2
$S_{a,min}$ = 3.3 kg/mm^2
GTAC with TL
ℓ = 14 mm $d\ell/dn$ =
1.3 μ/flight
Magnification 5000 x

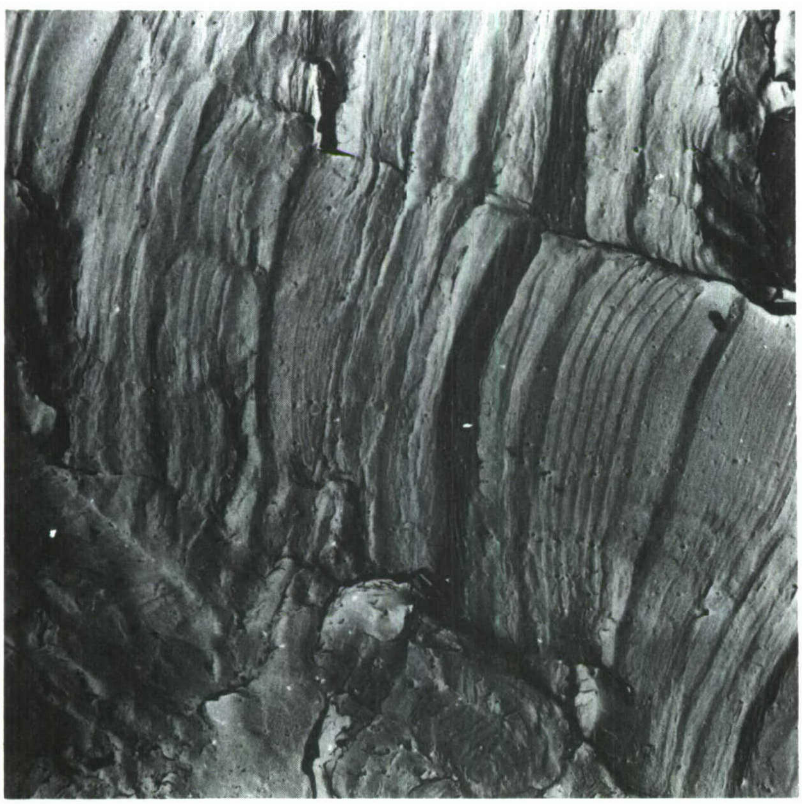

Specimen B18, 7075-T6
Programmed flight
simulation.
$S_{a,max}$ = 4.4 kg/mm^2
$S_{a,min}$ = 1.1 kg/mm^2
CTAC without TL
ℓ = 20 mm $d\ell/dn$ =
13 μ/flight.
Magnification 5000 x

Fig.19 Two examples of fatigue striations as observed by the electron microscope

Security Classification

DOCUMENT CONTROL DATA - R & D

(Security classification of title, body of abstract and indexing annotation must be entered when the overall report is classified)

1. ORIGINATING ACTIVITY (Corporate author) National Aerospace Laboratory NLR Amsterdam	2a. REPORT SECURITY CLASSIFICATION Unclassified
	2b. GROUP

3. REPORT TITLE

CRACK PROPAGATION IN ALUMINUM ALLOY SHEET MATERIALS UNDER FLIGHT-SIMULATION LOADING

4. DESCRIPTIVE NOTES (Type of report and inclusive dates)
Scientific. Final. 1 Sep. 1967 - 30 Nov. 1968

5. AUTHOR(S) (First name, middle initial, last name)

Schijve, J. , Jacobs, F.A. and Tromp, P.J.

6. REPORT DATE	7a. TOTAL NO. OF PAGES	7b. NO. OF REFS
September 1970	74	30

8a. CONTRACT OR GRANT NO. Contract F61052-67-C-0076	9a. ORIGINATOR'S REPORT NUMBER(S) NLR Tech.Report 68117
b. PROJECT NO. 1347-05	
c. 62405334	9b. OTHER REPORT NO(S) (Any other numbers that may be assigned this report)
d. 611347	

10. DISTRIBUTION STATEMENT

THIS DOCUMENT HAS BEEN APPROVED FOR PUBLIC RELEASE AND SALE ;
ITS DISTRIBUTION IS UNLIMITED.

11. SUPPLEMENTARY NOTES	12. SPONSORING MILITARY ACTIVITY
TECH, OTHER	Air Force Flight Dynamics Laboratory (FDTT) Wright-Patterson AFB, Ohio 45433

13. ABSTRACT

A large number of flight-simulation tests were carried out on sheet specimens of 7075-T6 and 2024-T3 clad material. A gust load spectrum was adopted and a flight-by-flight loading was applied. The investigation is essentially concerned with macro-crack propagation although a few exploratory tests were conducted on the crack nucleation period. The major trends emerging from tests with a variety of loading programs are: (1) The omission of taxiing loads from the ground-to-air cycles did not affect the crack propagation. (2) The sequence of the gust cycles in a flight (random, programmed, reversed gust cycles) did not have a significant influence on the crack propagation. (3) Omission of gust cycles with small amplitudes systematically increased the crack propagation life. (4) The most predominant effect on the crack propagation was coming from the maximum gust amplitude included in the test. Increasing this amplitude gave a large increase of the crack propagation life. (5) Application in each flight of a single gust load only, namely the largest upward gust load, increased the crack propagation life three times. (6) Omission of the ground-to-air cycle increased the life 1.5-1.8 times. The discussion and the analysis of the results include such aspects as fractographic analysis, possible mechanisms for interaction effects between load cycles of different magnitudes and damage calculations. The conclusions at the end of the report have a number of implications for testing procedures to be applied in full-scale testing aiming at crack propagation data for fail-safe considerations. A recommendation is made for selecting the maximum load level in such a test. Recommendations for further study are also made.

14. KEY WORDS	LINK A		LINK B		LINK C	
	ROLE	WT	ROLE	WT	ROLE	WT
Fatigue						
Crack propagation						
Random loads						
Flight-simulation loading						
Full-scale fatigue test						
Gust loads						
Taxiing loads						
Ground-to-air cycle						
Aluminum alloys						